BLIND DOCKING SIMULATIONS OF BENZOTHIAZOLES ON TRIOSEPHOSPHATE ISOMERASE

by

Gülgün Ural

B.S. in Chemical Enginneering, Hacettepe University, 2007

Submitted to the Institute for Graduate Studies in
Science and Engineering in partial fulfillment of
the requirements for the degree of
Master of Science

Graduate Program in Computational Science and Engineering

Boğaziçi University

2011

BLIND DOCKING SIMULATIONS OF BENZOTHIAZOLES ON TRIOSEPHOSPHATE ISOMERASE

APPROVED BY:

Prof. Pemra Doruker Turgut . . . . . .
(Thesis Supervisor)

Assist. Prof. Demet Akten Akdoğan . . . . . .
(Thesis Co-supervisor)

Prof. Viktorya Aviyente . . . . . .

Prof. Türkan Haliloğlu . . . . . .

Assist. Prof. Elif Özkırımlı Ölmez . . . . . .

DATE OF APPROVAL: 19.01.2011

ACKNOWLEDGEMENTS

In the first place I would like to express my sincere and deep gratitude to my thesis advisors, Prof. Pemra Doruker Turgut and Assist. Prof. Demet Akten Akdoğan, for their supervision, support and patience. Their understanding and personal guidance helped me at every stage of this thesis. It has been an honour and a privilege working with them.

I would like to thank my thesis committee members: Prof. Viktorya Aviyente, Prof. Türkan Haliloğlu, Assist. Prof. Elif Özkırımlı Ölmez for their time, interest and helpful comments.

My special thanks go to my friend and colleague Zeynep Kürkçüoğlu, it is a great pleasure to collaborate with her. She was always there to help out on issues throughout this thesis. I am indebted to her more than she knows.

Furthermore, I would like to extend my thanks to Arzu Uyar, Fidan Sümbül, Seren Soner, Pemra Özbek, Burcu Aykaç Fas, and Canan Dedeoğlu for their support during my thesis.

Words fail me to express my appreciation to my family: İsmail Ural, Gönül Ural and Yasemin Ural. I am very grateful to them for their love and persistent confidence in me.

ABSTRACT

BLIND DOCKING SIMULATIONS OF BENZOTHIAZOLES ON TRIOSEPHOSPHATE ISOMERASE

Selective inhibition of the activity of the glycolytic enzyme triosephosphate isomerase from Trypanosoma cruzi (TcTIM) as opposed to human TIM (hTIM) has been critical for drug design studies on Chagas disease. The aim of this docking study is to uncover the binding modes of benzothiazoles, reported as effective inhibitors of TcTIM. Blind dockings of five benzothiazoles are performed on both TcTIM and hTIM by using the Lamarckian genetic algorithm of AutoDock v4.0. Protein flexibility is incorporated via docking to multiple, distinct conformations that are obtained from extended molecular dynamics simulations. The clusters that fall within 1 kcal/mol of the lowest energy poses from docking are analyzed for determination of alternative binding sites. The inhibitors mostly bind to the tunnel-shaped region formed at the interface of the subunits in TcTIM, whereas other sites are preferred by the non-inhibitors. Moreover, blind dockings to equilibrated conformers of TcTIM monomer indicate no distinct tendency of inhibitors for binding to the interface region that becomes solvent accessible upon dissociation to monomers. Thus, the tunnel-shaped cavity on the TcTIM dimer interface is the most distinct site for the action of inhibitors, consistent with previous studies. Interactions of strong inhibitors at the interface at the TcTIM interface include π-π interactions with aromatic residues (Phe75, Tyr102 and Tyr103) and cation-π interactions (with Arg71, Arg99 and Lys113). In addition, multiple hydrogen bonds between the sulfonate group (present only in inhibitors) and residues Asn67, Thr70, Arg99 and Lys113 are found to be specific in the case of the strong inhibitors. Further blind dockings of sulfonate-free derivatives of inhibitors and a sulfonate-added derivative of a non-inhibitor on TcTIM have indicated that the sulfonate group aids the correct positioning of benzothiazoles in the tunnel-shaped cavity. The inhibitors docked on hTIM conformers show a non-selective behavior for the interface of hTIM dimer, which does not present an accessible tunnel-shaped cavity as TcTIM. Binding sites other than the interface region are also reported for TcTIM and hTIM.

ÖZET

BENZOTİYAZOLLERİN TRİOZ FOSFAT İZOMERAZ ÜZERİNDE YERLEŞTİRME SİMULASYONLARI

Trypanosoma cruzi ‘de bulunan glikolitik enzim trioz fosfat izomeraz’ın (TcTIM), insana ait trioz fosfat izomeraz’ı (hTIM) etkilemeyecek şekilde olan seçici inhibasyonu, Chagas hastalığna karşı ilaç geliştirme çalışmalarında kritik bir noktadır. Bu tezde uygulanan yerleştirme çalışmalarının amacı, TcTIM’i inhibe eden benzotiyazollerin, enzime bağlanma modlarını ortaya çıkarmaktır. Beş benzotiyazolün TcTIM ve hTIM üzerine yerleştirme çalışmaları, Autodock v.4 paket programının Lamarckian Genetik Algoritması kullanılarak yapılmıştır. Moleküler dinamik simulasyonlardan enzimin farklı konformasyonları alınarak, protein esnekliği çalışmalara dahil edilmiştir. Ligandların bağlanma konumlarının belirlenmesi için, en düşük enerjili konformasyon ve onun 1 kkal/mol yakınında bulunan konformasyonlar analiz edilmiştir. Etkili ligandlar bağlanmak için genelde TcTIM’in arayüzeyinde bulunan tünel şekilli kısmı tercih ederken, etkisiz ligandların enzimin başka kısımlarına bağlandığı gözlemlenmiştir. TcTIM monomer üzerinde yapılan yerleştirme çalışmalarının sonuçlarına gore, etkili ligandların dimerin ayrışması sırasında açık hale gelen arayüzey bölgesine bağlanma eğilimleri çok yüksek değildir. Bu yüzden önceki çalışmalarla uyumlu olarak, TcTIM dimerin arayüzeyinde bulunan tünel şekilli kısmın etkili ligandlar için başlıca bağlanma yeri olduğu görülmüştür. Etkili ligandlar ile enzim arasında π-π etkileşimleri (Phe75, Tyr102 ve Tyr103 rezidüleri ile), katyon-π etkileşimleri (Arg71, Arg99 ve Lys113 rezidüleri ile) vardır. Ayrıca, etkili ligandlara ait sülfonat grubunun Asn67, Arg99 and Lys113 rezidüleri ile yaptığı çoklu hidrojen bağları TcTIM dimer için spesifiktir. Etkili ligandların sülfonat içermeyen türevleri ve etkisiz ligandın sülfonat içeren türevi ile TcTIM dimer üzerinde yerleştirme çalışmaları, sülfonat grubunun ligandların arayüzey üzerindeki tünel şekilli kısımda doğru yerleşmelerine yardımcı olduğununu göstermiştir. hTIM dimer üzerindeki yerleştirme çalışmalarında, etkili ligandlar arayüzey bölgesi (ulaşılabilinen tünel şekilli kısım yoktur) için seçici değillerdir. Bu çalışmada TcTIM ve hTIM üzerinde, arayüzeyden farklı olan bağlanma yerleri de gösterilmiştir.

TABLE OF CONTENTS

LIST OF FIGURES

LIST OF TABLES

LIST OF SYMBOLS/ABBREVIATIONS

2D	Two-dimensional
a_i	Acceleration of an atom i
F_i	Force on particle i
f_i	The fitness of the individual
f_w	The fitness of the worst individual
$\langle f \rangle$	The mean fitness of the population
k_{li}	Force constant that describes the stiffness of the specific bond
$k_{\theta i}$	The stiffness of the bond angle
l_{li}	Instantaneous bond length
$l_{i,0}$	Equilibrium length of a bond
m_i	Mass of particle *i*
N	Number of Particles
q_i, q_j	Charges of atoms
P	Pressure
R_i	Position vector of residue i
r_{ij}	The distance between partial charges
T	Temperature
t	Time
$\mathbf{v}_i$	Velocity of an atom i
ΔG	The estimated free energy of binding
Å	Angstrom
α	Alpha helix
β	Beta strand
γ_i	Phase factor
γ	Uniform Hookean force constant
ε_{ij}	Well depth
ε_0	The permittivity of the free space
ε_r	Relative permittivity
θ_i	Instantaneous angle

$\theta_{i,0}$	Equilibrium angle
σ_{ij}	Lennard-Jones collision parameter
φ_i	The instantaneous torsional angle

Ala	Alanine
Arg	Arginine
Asn	Asparagine
Asp	Aspartic Acid
Cys	Cysteine
DHAP	Dihydroxyacetone phosphate
GAP	D-glyceraldehyde 3-phosphate
Gln	Glutamine
Glu	Glutamic Acid
Gly	Glycine
His	Histidine
hTIM	Triosephosphate isomerase from human
Leu	Leucine
Lys	Lysine
MD	Molecular Dynamics
Met	Methionine
NMR	Nuclear Magnetic Resonance
PDB	Protein Data Bank
PGH	Phosphoglycolohydroxamate
Phe	Phenylalanine
Pro	Proline
RMSD	Root mean square deviation
SASA	Solvent accessible surface area
Ser	Serine
TcTIM	Triosephosphate isomerase from *Trypanosoma Cruzi*
Thr	Threonine
TIM	Triosephosphate isomerase
Trp	Tryptophan
Tyr	Tyrosine

1. INTRODUCTION

Chagas Disease is a serious illness caused by the parasite *Trypanosoma cruzi* that has affected over 20 million people in Latin America during 1980s. The number of infected people has recently decreased to 9 million (mostly children) with the effort of affected countries to control the disease (World Health Organization). However, the disease still poses a threat to Latin America as well as to other parts of the world like Europe, USA and Canada in consequence of infected blood and blood products used in blood transmission and organ transplantation. The disease has a symptomless acute phase immediately after the infection, and a chronic phase showing up 15 or 20 years later. The heart, esophagus, lower intestine, and peripheral nervous system are affected in the chronic phase, for which there is not any efficient treatment. To fight the disease, drug discovery studies have focused on the parasite-specific inhibition of the enzyme triosephosphate isomerase (TIM) which plays an important role in the glycolytic pathway in nearly all organisms (Tellez-Valencia *et al.,* 2002, Espinoza-Fonseca and Trujilo-Ferrara, 2005, Olivares-Illana *et al.,* 2007, Gayosso-De-Lucio *et al.,* 2009).

In most of the species that perform glycolysis, TIM is a dimer formed by two identical monomers. TIM shows full activity in dimer form, despite the fact that each monomer has its own catalytic site (Schnackerz and Gracy, 1991, Zomosa-Signoret *et al.,* 2003). TIM exists in both human and parasite, therefore it becomes crucial to inhibit the activity of TIM from *Trypanosoma cruzi* (TcTIM) but not human TIM (hTIM). The activity and the stability of the dimer are connected to intersubunit contacts that occurs at the interface between monomers (Mainfroid *et al.,* 1996). Generally, the residues that form the interface region of oligomeric enzymes are less conserved than the residues in the active sites. Hence, the interface region becomes an important target area for designing new drug molecules that would specifically bind and inhibit an oligomeric enzyme from a given species. (Perez-Montfort *et al.,* 2002). As a result, drug design studies on TcTIM dimer have aimed to disrupt the interface and not the active site of the enzyme.

Previously, benzothiazoles have been reported to be drug canditates for inactivation of TcTIM and it was experimentally shown that these potent inhibitors affect TcTIM's activity, but not hTIM's except at high concentrations (Tellez-Valencia *et al.,* 2002).

In drug design studies, automated docking is generally used to find the bound conformation of a small molecule (ligand) to a macromolecular target of known structure. Conformational dynamics and flexibility of molecules are key aspects that determine biological activity.

In the present study, docking to different conformers of TcTIM and hTIM was employed to incorporate flexibility. Five ligands that were chosen from reported benzothiazoles list (Tellez-Valencia *et al.,* 2002) were used in dockings. In these dockings protein held rigid whereas ligand was flexible.

In chapters 4.1 and 4.2, blind docking methodology was employed for both TcTIM dimer and monomer. Two and three conformes were taken from MD simulations for TcTIM monomer and TcTIM dimer, respectively. Instead of targeting only the interface region as in the case of previous studies (Espinoza-Fonseca and Trujilo-Ferrara, 2004, 2005, 2006), blind docking is implemented to identify the selectivity of the benzothiazoles for the interface region of the dimer. Blind monomer dockings are also attempted to understand whether inhibitors bind more preferentially to dimer interface or to the monomer. In both cases, the presence of the inhibitor could prevent the formation of a stable interface for the dimer. In chapter 4.3, the significiance of the sulfonate group in the inhibition process was also investigated through dockings of sulfonate-free inhibitor derivatives and a sulfonate added non-inhibitor derivative, on a TcTIM dimer conformer. Chapter 4.4 consists in blind docking experiments are performed using three hTIM dimer conformers from MD simulation, in order to reveal the differences between binding poses of most potent inhibitor ligands on TcTIM and hTIM.

2. TRIOSEPHOSPHATE ISOMERASE

Triosephosphate isomerase (TIM) is a crucial enzyme in glycolysis that is going to be the target in the docking studies in this thesis. TIM is a homodimeric enzyme, which catalyzes the interconversion of dihyroxyacetone phosphate (DHAP) and D-glyceraldehyde 3-phosphate (GAP) (Albery and Knowles, 1976). Native TIM is formed of two identical monomers which are made up of eight central β-strands that are surrounded by eight α-helices. Specifically, each monomer adopts an $(\alpha/\beta)_8$ fold, generally named as the TIM barrel.

1.1 Structure of Triosephosphate Isomerase from *Trypanosoma Cruzi*

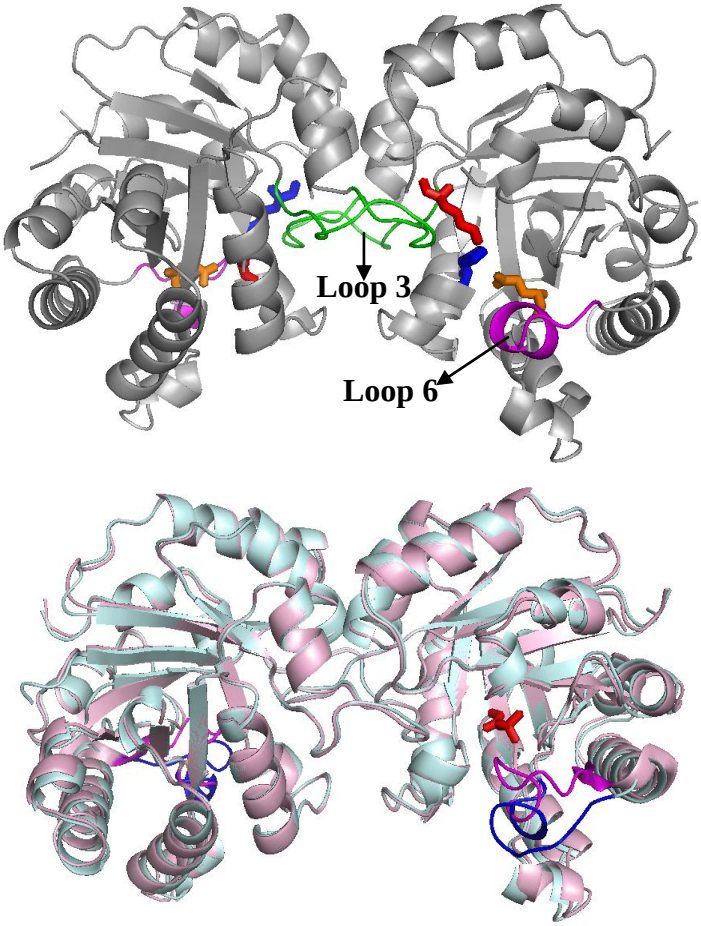

Figure 2.1. (a) X-ray structure of TcTIM, (b) Aligned structures of free (8TIM-Light blue) and bound (1TPH-Light pink) chicken TIM structures.

TcTIM also shows the characteristic α/β barrel structure of and its identical subunits (monomers) are chain A and chain B each comprises 249 residues. In Figure 2.1 (a) the x-ray structure for apo form of TcTIM is shown. The residues of the active site in TcTIM are

Lys14, His96 and Glu168 and shown in red, blue and orange stick representation, respectively. Their conformational arrangement in TcTIM is almost same with those of human TIM. However, side-chain of Glu168 in TcTIM shows difference in the orientation (Maldonado *et al.,* 1998). Loop 6 is shown in blue: open/apo conformation and magenta: closed/bound conformation. Ligand (PGH) is shown in red stick representation (Figure 2.1). Loop 6 that comprises residues Trp171 to Val178 in TcTIM, has a significant role in catalytic activity. Particularly, loop 6 closes over the bound ligand by covering the catalytic center during reaction and ligand is prevented from solvent exposure by this loop closure which is illustrated by Figure 2.1 (Wierenga *et al.,* 1991). However, this motion is not ligand- gated, loop 6 can also open and close in apo form (Williams and McDermott, 1995). Loop 6 (residues Pro166-Ala176 in chicken TIM) has highly conserved amino acid sequence that contains three hinge residues each at the N- and C- termini and it has been shown (on chicken TIM) that catalysis has been affected oppositely by the mutation of these hinge residues (except Pro166) to Gly (Xiang *et al.*, 2004; Kempf *et al.*, 2007).

Loop 3 **(**in Figure 2.1, residues 66 to 79, green) forms an important segment of the interface and surrounds the Cys15 that belongs to the other subunit. Disruption of the interface region formed by Cys15 and loop 3 of the other monomer has lead to the inhibition of catalytic activity (Olivares-Illana *et al.,* 2007).

1.2 Triosphosphate Isomerase from Trypanosoma Cruzi as a drug target

Considering the significant role of TIM in the glycolytic pathway, research groups have proposed some benzothiazole derivatives for the inhibition of TcTIM activity. In Table 2.1 these benzothiazoles and their inactivation percentages are shown (Tellez-Valencia *et al.,* 2002). Among the reported ten benzothiazloes (Table 2.1), five benzothiazoles were chosen to be studied in this thesis. Ligands 2 and 3 (do not have inhibitory effect on TcTIM), ligands 8,9 and 10 (inhibitors with the highest inactivation percentages, 95%, 91% and 95%, respectively) were selected in order to compare binding modes of inhibitors and non-inhibitors.

Table 2.1. Effect of some benzothiazoles on TcTIM. Flexible bonds of the used ligands are shown with red arrows (Tellez-Valencia *et al.*, 2002)

Ligand	Structure and flexible bonds	Inactivation %
1	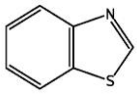	25
2	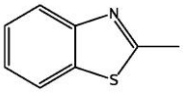	0
3	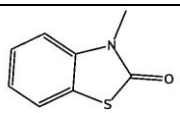	0
4	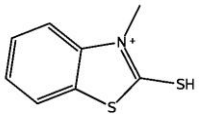	14
5	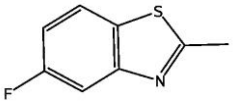	4
6	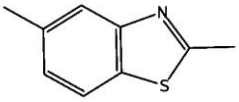	47
7	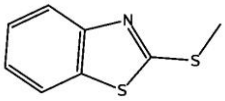	8
8	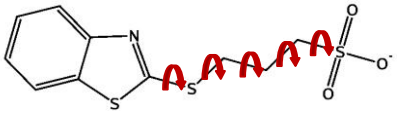	95
9	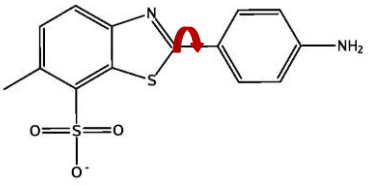	91
10	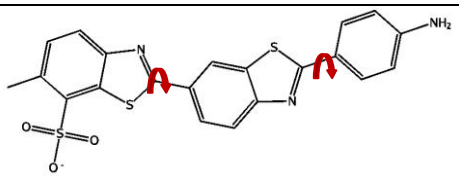	95
V7	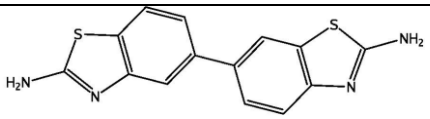	91

Compared to ligands 8, 9 and 10, ligands 1, 4, 5, 6 and 7 have lower inactivation percentages that are 25%, 14%, 4%, 47% and 8%, respectively (Table 2.1). In other words, they have not detrimental effect on TcTIM as much as ligands 8, 9 and 10 have. Therefore, these ligands were not be selected to study in this thesis.

Table 2.1 shows that, most potent inhibitors of TcTIM have a bulky group at the same position (C2) and a sulfonate group in their chemical structure. It has been claimed that the sulfonate group might have a role in molecular recognition by favoring interactions between ligands and enzyme because there are positively charged residues on loop 3 and on the interface (Tellez-Valencia *et al.,* 2002). However, later studies claimed that benzothiazole moiety is necessary for molecular recognition (Espinoza-Fonseca and Trujilo-Ferrara, 2004). As a result of these studies the role of the sulfonate group in inhibition process remains unknown.

It was experimentally shown that the benzothiazoles inhibit TcTIM's activity but not hTIM's except at high concentrations. In Table 2.2 the IC_{50} values (concentrations that cause half-maximal inactivation) are listed for ligands 8,9 and 10 (benzothiazoles with highest inhibitory effects) on TIMs from different species (Tellez-Valencia *et al.,* 2002).

Table 2.2. The IC_{50}s for ligands 8,9 and 10 on TIMs from T.cruzi (TcTIM), human (hTIM), and the M15C mutant of human TIM (M15ChTIM) (Tellez-Valencia *et al.,* 2002)

Compound	TcTIM	hTIM	M15ChTIM
8	33 μm	422 μm	120 μm
9	56 μm	3.3 mM	321 μm
10	8 μm	1.6 mM	74 μm

According to the Table 2.2, relatively low concentrations of ligands 8,9 and 10 (in μm range) inhibit TcTIM compared to hTIM. This situation might be related to the structural differences between TcTIM and hTIM. One of those differences is TcTIM has a cysteine (Cys15) at the interface, whereas hTIM has a methionine (Met15) at the same position. The effect of the cysteine existing in position 15 was investigated via studies on a mutant of hTIM (M15ChTIM) in which the Met15 was replaced by cysteine. The results showed that the mutant enzyme is more sensitive to ligands 8, 9 and 10 (Table 2.2-last

column). Therefore, Cys15 at the interface is related with the detrimental action of the ligands (Tellez-Valencia *et al.,* 2002). In all TIM's, side chain of residue 15 of one monomer is near the residues of loop 3 of the other monomer and loop 3 has a important role in conserving stability of the dimer and catalysis (Gomez Puyou *et al.,* 1995, Mainfroid *et al.,* 1996, Schliebs *et al.,* 1997, Garza-Ramos *et al.,* 1996, Hernandez-Alacantara *et al.,* 2002). Hence, the interactions due to the positioning of Cys15, are regarded as target for drug design studies (Tellez-Valencia *et al.,* 2002). However, experimental study with TcTIM and the mutants (in which TcTIM's cysteine residues were replaced with valine or alanine) later claimed that Cys15 does not essentially play a role in the inhibition process, the inhibition might be related to TcTIM's higher intrinsic flexibility and disruption of the interactions between its two subunits (Olivares-Illana *et al.,* 2007).

Another structural difference between TcTIM and hTIM is the packing of the interface residues . In hTIM the interface is more tightly packed compared to TcTIM, i.e. less accessible (Espinoza-Fonseca and Trujilo-Ferrara, 2005, Espinoza-Fonseca and Trujilo-Ferrara, 2006).

In former "rigid protein-flexible ligand" computational docking studies, seven benzothiazoles (ligands 1, 4, 6, 7, 8, 9, and 10) in table 2.1, were docked to TcTIM and hTIM interfaces, in order to reveal the differences in binding modes and affinities (Espinoza-Fonseca and Trujilo-Ferrara, 2004 and 2005). The dockings were performed on a receptor conformer obtained via energy minimization for both TcTIM and hTIM. Moreover, another benzothiazole called "compound V7" (Table 2.1), that selectively inhibits TcTIM (Olivares-Illana *et al.,* 2006), was docked on six different species' receptor conformation, after been equilibrated via 1.5 ns MD simulation (Espinoza Fonseca and Trujillo Ferrara, 2006). In all these dockings, only the interface region was targeted. The authors emphasized the importance of aromatic clusters at the interface in both hTIM and TcTIM, since the favorable orientation of aromatic rings might lead to π-π and cation-π interactions (aromatic interactions). It is claimed that the dimer disruption might take place due to these strong interactions (Espinoza-Fonseca and Trujilo-Ferrara, 2004).

The aromatic clusters of hTIM are formed by Phe74 and Tyr67 from one monomer and by Phe102 from other monomer, whereas aromatic clusters of TcTIM are made up of Phe75 from one monomer, Tyr102 and Tyr103 from the other monomer. The conformational arrangement of these aromatic clusters determines the accesibility of the interface region. Inhibition effect of benzothiazoles is related with easy access to the region, since this would lead to the disruption of the interaction with loop 3, that is crucial for conserving the stability of the dimer form. For instance, in hTIM the conformational distribution Tyr67-Phe74-Phe102 restricts the accessibility to this region, thus large benzothiazoles that have inhibitory effect cannot be accomodated in hTIM interface. However in TcTIM, the packing of aromatic clusters forms easily accessible cavity at the interface (Figure 2.2), thus the inhibition effect of benzothiazoles on TcTIM might be related to this structural difference (Espinoza-Fonseca and Trujilo-Ferrara, 2005).

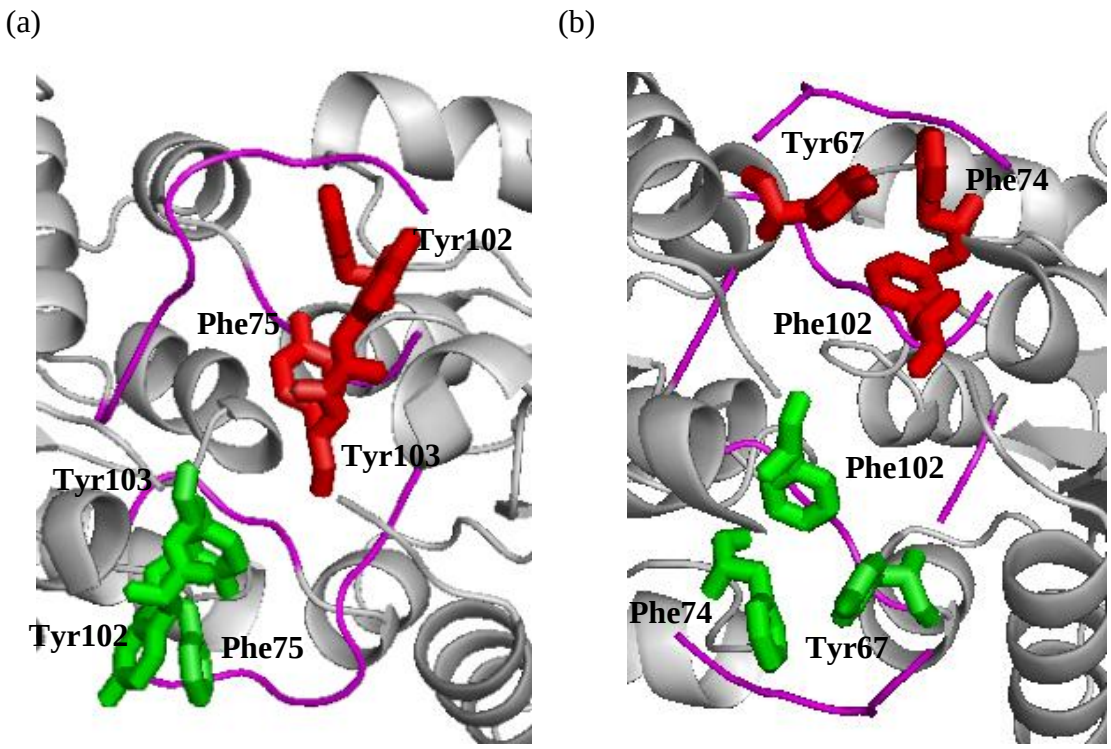

Figure 2.2. The representation of aromatic clusters in (a) TcTIM and (b) hTIM, loop 3 is shown in cartoon representation (magenta)

The earlier experimental studies on TcTIM showed that detrimental effect of the benzothiazoles takes place during the dissociation and association of the monomers, rather than the transformations of inactive to active dimer (Tellez-Valencia *et al.,* 2002). In order

to understand the nature of the inhibition process, ligands and their interactions with both monomer and dimer forms of the TcTIM are investigated via ensemble docking experiments in the present study.

1.3 Incorporation of protein flexibility in docking studies

Protein's flexibility has significant role in determining the interaction of proteins with ligands and other molecules. In recent docking studies on TcTIM, main chain flexibility of the protein has not been considered (Espinoza-Fonseca and Trujilo-Ferrara, 2004, 2005, 2006). However, it needs to be taken into account in order to obtain more accurate and realistic interpretations. Previously, using multiple conformations was announced to be an equivalent of flexible protein docking and ensembles of NMR and X-ray structures were used as target structures (Knegtel *et al*., 1997). In this respect, multiple receptor conformations ("ensemble docking" algortihms) might be used to get a feasible set of conformations representing the bound, the unbound and the intermadiate states of the protein. There are various methodologies to produce conformational ensembles for docking, such as normal mode analysis (Cavasotto and Kovacs, 2005), molecular dynamics (Zacharias, 2004) and Monte-Carlo simulations (Gray *et al.*, 2003, Cavasotto and Abagyan, 2004). By means of these techniques, the importance of conformational variations in a specific region on the protein might be revealed.

3. COMPUTATIONAL METHODOLOGY

The basic features of the computational methods used in this study, that are molecular dynamics simulations and docking, are introduced in the following section.

3.1 Molecular Dynamics Simulations

Molecular Dynamics(MD) simulation is a useful computational method to analyze the equilibrium and dynamic properties of macromolecules, such as their conformational behavior and molecular interactions. MD simulation is based on Newton's second law or the equation of motion. The acceleration of each atom in the system can be determined by means of the total force acting on it. The integration of the equations of motion produce a trajectory that decribes evolution of the positions, velocities and accelerations of the particles with time. Equation of motion applies to each atom in the system :

$$\frac{d^2 \mathrm{R_i}}{dt^2} = \frac{\mathrm{F}_i}{m_i} \tag{3.1}$$

Here, R_i represents the position of particle i, and F_i is the total force acting on particle i exerted by all other molecules, and m_i its the molecular mass.

3.1.1. Force Field

The empirical formula describing the potential energy surface is called the force field. Force fields use internal coordinates of the particles to describe the bonded interactions (bond lengths, bond angles, torsion angles) of the potential energy surface, and inter-atomic distances to describe the non-bonded interactions (van der Waals and electrostatic) between atoms. Thus, the potential energy surface can be described by an equation containing the following basic terms.

$$V(R_1,....,R_N) = \sum_{bonds} \frac{k_{li}}{2}(l_{li} - l_{i,0})^2 + \quad \text{“Bond Streching”}$$

$$\sum_{angles} \frac{k_{\theta i}}{2}(\theta_i - \theta_{i,0})^2 + \quad \text{“Angle Bending”} \qquad (3.2)$$

$$\sum_{torsions} \frac{V_n}{2}(1 + \cos(n\phi_i - \delta_i)) + \quad \text{“Bond Rotation(torsion)”}$$

$$\sum_{i=1}^{N}\sum_{j=i+1}^{N}\left(4\varepsilon_{ij}\left[\left(\frac{\sigma_{ij}}{r_{ij}}\right)^{12} - \left(\frac{\sigma_{ij}}{r_{ij}}\right)^{6}\right] + \frac{q_i q_j}{4\pi\varepsilon_0 r_{ij}}\right) \quad \text{“Nonbonded Interactions”}$$

Here, $V(R_1,.....,R_N)$ indicates the total potential energy, which is a function of the positions (R_i) of N atoms. The first term in equation is the potential energy due to the changes of the bond length connecting two atoms. The bond streching equation is based on Hooke’s Law, is for a simple harmonic spring. The k_{li} parameter represents the stiffness of the bond spring. l_{li} and $l_{i,0}$ define instantaneous and the equlibrium lengths of the bond, respectively. The second term, which is also based on Hooke’s Law, describes the energy due to the vibration about the equlibrium bond angle. The constant $k_{\theta i}$ represents the stiffness of the bond angle. θ_i and $\theta_{i,0}$ are the instantenous and the equilibrium angle of the bond, respectively. The third term represents the torsion energy for a rotating bond. V_n is a qualitative indication of the relative barriers to rotation, δ is the phase factor that determines the location of torsional angle is minima, ϕ is the instantaneous torsional angle. The last term defines the non-bonded interactions consisting of two different potentials. The former one is the Lennard-Jones 12-6 potential function that represents van der Waals interactions and it includes a repulsive term dominant at short distances and an attractive term for dispersion forces that are always present. r_{ij} is the distance between the atoms i and j. ε_{ij} (well depth) and σ_{ij} (the collision diameter) are adjustable parameters. Van der Waals attraction occurs at relatively short distances and rapidly dies off when the interacting atoms move apart by several Angstroms. The second equation is the Coulomb potential for electrostatic interactions between charged particles. The parameters q_i, q_j are partial charges of the atoms, ε_0 is the permittivity of the free space and ε_r is the relative permittivity. Non-bonded terms are formed by a double summation (Leach,2001).

3.1.2. Initialization of the System

Periodic boundary conditions are used in MD simulations, to define boundary effects in the simulation. Thus, the surface effect can be eliminated for all system sizes. To apply periodic boundary conditions, the protein is enclosed in a solvent box that is replicated to infinity by rigid translation in all the three Cartesian directions. A two dimensional periodic box is shown in Figure 3.1.As a particle leaves a cell, its image enters from the adjoining copy that is indicated by the vector displacements in the figure. This keeps the number of particles constant in the central box. The shape of the solvent box may be a truncated octahedron, a cube or a hexagonal prism according to the shape of the protein.

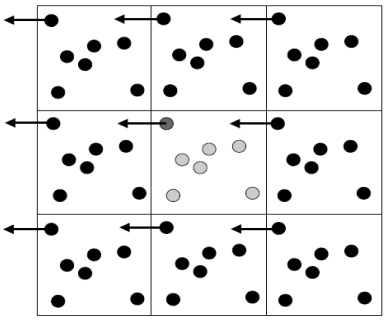

Figure 3.1. Small part of the molecular ensemble in two dimensional periodic box

Energy minimization before MD simulation, is applied to find the configuration of the system at a local energy minimum and to prevent any high-energy interactions in the system, that might cause instabilities during simulation. Minimization leads to a more stable starting conformation and removes the steric clashes in the system.

In order to perform an MD simulation, it is essential to determine an initial configuration of the system by specifying 3N atomic coordinates (R_i) at the initial time (t=0). The initial configuration can be generated by using experimental data, such as a crystal structure. After the initial configuration of the system is minimized in a solvent box, the initial velocities are assigned according to the Maxwell-Boltzmann distrubution at the initial temperature (Leach, 2001).

3.1.3. Integration Algorithm

After setting up the system (putting the protein in a solvent, assigning initial positions and velocities), the potential energy of the system can be calculated and then the force on each atom can be determined.

$$\mathrm{F}_i = -\nabla V_i(\mathrm{R}_1,...,\mathrm{R}_N) = -\frac{\partial V(\mathrm{R}_1,...,\mathrm{R}_N)}{\partial \mathrm{R}_i} \tag{3.3}$$

When the forces on each atom at the current time step are calculated, new positions can be generated according to the equation 3.1. There are several algorithms that are used to perform the integration of equation 3.1. The integration is seperated into many small time stages by a fixed time Δt and all algorithms assume that the positions and the dynamic properties (velocities(v_i), accelerations(a_i)) can be approximated using Taylor series expansions. One of such algorithm is the Verlet algorithm (Verlet, 1967), that utilizes positions (R_i) and accelerations (ai) at time t, and the positions from the previous step R_i (t-Δt), to calculate the new positions at t+Δt, $R_i(t+\Delta t)$.

$$\mathrm{R}_i(t+\Delta t) = \mathrm{R}_i(t) + \mathrm{v}_i(t)\Delta t + \frac{1}{2}\mathrm{a}_i(t)\Delta t^2 + \cdots \tag{3.4}$$

$$\mathrm{R}_i(t-\Delta t) = \mathrm{R}_i(t) - \mathrm{v}_i(t)\Delta t + \frac{1}{2}\mathrm{a}_i(t)\Delta t^2 - \cdots \tag{3.5}$$

Adding these equations together yields :

$$\mathrm{R}_i(t+\Delta t) \approx -\mathrm{R}_i(t-\Delta t) + 2\mathrm{R}_i(t) + \Delta t^2 \mathrm{a}_i\,(t) \tag{3.6}$$

The velocities can be calculated by dividing the difference of the positions at t-Δt and t+Δt by 2Δt:

$$v_i(t) \approx \frac{1}{2\Delta t}\left[\mathrm{R}_i(t+\Delta t) - \mathrm{R}_i(t-\Delta t)\right] \tag{3.7}$$

In order to increase the accuracy in caluculations of positions and velocities, variations of the Verlet algorithm have been proposed, such as Leap-frog (Hockney,1970) algorithm and the velocity Verlet method (Swope *et al.*, 1982) that is used in MD simulations for this thesis. In this algorithm, positions, velocities and accelerations at time

t+Δt are obtained from the same quantities at time t. Furthermore, this method does not involve precision (Leach 2001).

$$\mathrm{R}_i(t+\Delta t) = \mathrm{R}_i(t) + v_i(t)\Delta t + \frac{1}{2}a_i(t)\Delta t^2 \tag{3.8}$$

$$v_i(t+\Delta t) = v_i(t) + \frac{1}{2}\Delta t\left[a_i(t) + a_i(t+\Delta t)\right] \tag{3.9}$$

The algorithm is applied as a three stage procedure, since as seen from equation (3.8), the accelerations at both t and t+Δt is required to calculate the new velocities. Firstly, positions at t+ Δt are calculated according to equation (3.7) and the velocities at time t+Δt/2 are evaluated by using the following equation:

$$v_i(t+\frac{\Delta t}{2}) = v_i(t) + \frac{1}{2}\Delta t a_i(t) \tag{3.10}$$

Then, forces are computed from the current positions to obtain a(t+ Δt). In the final step, the velocities at time time t+ Δt are calculated:

$$v_i(t+\Delta t) = v_i(t+\frac{1}{2}\Delta t) + \frac{1}{2}\Delta t a_i(t+\Delta t) \tag{3.11}$$

3.1.4. Molecular Dynamics Simulations for Conformer Generation

In this thesis MD simulations were carried out for monomeric and dimeric forms of TCTIM and the dimeric form of hTIM to obtain well-equilbrated conformers for ensemble docking experiments. The crystal structure of apo TcTIM dimer at 1.83 Å resolution and holo hTIM dimer at 2.8 Å resolution were obtained from the Protein Data Bank with respective PDB codes: 1TCD (Maldonado *et al.,* 1998) and 1HTI (Mande *et al.,* 1994)) The parameters used in the simulations are listed in Table 3.1.

Table 3.1. Molecular dynamics simulation parameters for TcTIM monomer, dimer and hTIM dimer

	TcTIM Monomer	TcTIM Dimer	hTIM Dimer
Software Type	NAMD v2.6	AMBER	NAMD v2.6
Forcefield	CHARMM	ff03	CHARMM
Simulation time	20 ns	13.4 ns	55 ns
Temperature	310 K	300 K	310 K
Pressure	1 atm	1 atm	1 atm
Time step	2 fs	2 fs	2 fs
Periodic Box	52.4 -67.7 -72.1 Å	89.2 Å	65.8 -96.6 -84.1 Å

3.1.4.1. TcTIM Monomer Run

Chain A of TcTIM was extracted from the dimer's crystal structure, was equilibrated via energy minimization and MD simulation using NAMD v2.6 simulation package (Philips et al., 2005) before selecting the distinct target structures from the production phase of the trajectory for further docking studies. MD simulation was performed at constant NPT at 310 K using Langevin dynamics for all non-hydrogen atoms, with a Langevin damping coefficient of 5 ps-1. The system was kept at constant pressure of 1 atm by using a Nose-Hoover Langevin piston (Feller et al., 1995) with a period of 100 fs and damping timescale of 50 ps. To simulate the cytoplasmic enviroment, the system was first solvated in a water box with dimensions 52.4 Å-67.7 Å-72.1 Å (Table 3.1) and ions were added to make the overall system neutral using the plug-ins of VMD molecular visualization program (Humphrey et al., 1996). CHARMM22 forcefield (MacKerell et al., 1992, 1998) was used to describe the interaction potential of the protein and waters were treated explicitly using TIP3P model (Jorgensen et al., 1983).

Long-range electrostatic interactions were treated by the particle mesh Ewald (PME) method (Essman *et al.,* 1995) with a grid point density of over 1/Å. A cut off of 12 Å was used for van der Waals and short-range electrostatic interactions with a switching function. Time step was set to 2 fs by using SHAKE algorithm (Ryckaert *et al.,* 1977) for bonds

involving hydrogens and the data was recorded every 1 ps. The number of time steps between each full electrostatics evaluation was set to 2. Short-range non-bonded interactions were calculated at every time step. Prior to 20 ns of MD simulation, the system was subjected 10,000 steps of energy minimization using conjugate gradient algorithm.

3.1.4.2. TcTIM Dimer Run

The dimer simulation was performed using the AMBER (Case *et al.*, 2004, 2005) simulation package with the ff03 forcefield parameters (Duan *et al.*, 2003). The protein was solvated in a periodic truncated octahedron box with dimensions of 89.2 Å in explicit TIP3P water molecules. Energy minimization was carried out via 50 cycles of steepest descent algorithm, followed by conjugate gradient till the RMS gradient per atom reached 0.01 kcal/mol/ Å. An NPT Simulation at 300 K and 1 atm was performed using the weak coupling algorithm for both pressure and temperature (Berendsen *et al*. 1984). The Ewald summation technique with the particle-mesh method (Essman *et al.*, 1995) was applied for long-range electrostatic interactions. The simulation was carried out for 13.4 ns with a time step of 2 fs with the application of SHAKE algorithm (Ryckaert *et al.*, 1977).

3.1.4.3. hTIM Dimer Run

Same procedure as in TcTIM monomer run was applied to the crystal structure of hTIM dimer using NAMD v2.6. The periodic box dimensions were 65.8 Å x 96.6 Å x 84.1. In as much as a relatively longer run of 55 ns duration was performed.

3.1.5. Conformer Selection from MD Simulations for Dockings

For monomer dockings, two snapshots at 14 and 20 ns (denoted as M1 and M2) were selected with M2 being the last snapshot of the monomer simulation. The snapshot M1 has the highest root mean square distance (RMSD = 1.13 Å) with respect to M2 after structural alignment based on the backbone atoms.

For TcTIM dimer dockings, three snapshots were selected at 6.8, 10.5 and 13.4 ns (D1, D2 and D3). The last snapshot (D3) exhibits RMSD values of 1.38 and 1.47 Å with respect to D1 and D2. RMSD between D1 and D2 is 1.25 Å.

The selection of conformers for hTIM was based on k-means clustering (Lloyd, 1982) based on the RMSD values. First 6 ns of the MD simulation were discarded for equilibration. The clustering was performed by using the MMTSB tool set (Feig *et al*., 2001). The conformations were clustered according to 2 Å RMSD, with respect to the centroids (average) structure in each cluster leading to three clusters with 988, 575 and 71 elements. One representative snapshot was taken from each cluster for blind docking. These snapshots named as H1 (at 20 ns-member of 2nd cluster), H2 (at 21.7 ns-member of 1st cluster) and H3 (at 35.8 ns-member of 3rd cluster) have the lowest RMSD value with respect to the centroid structure in the corresponding clusters.

3.2 Docking Tool: Autodock Version 4.0

As the docking tool, the genetic algorithm of Autodock v4.0 was utilized (Morris *et al.,* 2009). Autodock is a docking tool to simulate the interactions between small flexible ligands and macromolecules of known structure. Moreover, it's a freeware with grid-based method for energy evaluation (Morris *et al.,* 1998). In this section, information will be given about the genetic algorithm and the scoring function employed in docking

3.2.1. Genetic Algorithm

Genetic algorithms are used to search conformational space by mutating a ligand so that its lowest energy conformation in the environment of a fixed protein can be found. Specifically, genetic algorithm is based on evolutionary biology, related with the concepts of natural selection, inheritance, mutation and crossover (Hetenyi *et al.,* 2002).

In the Lamarckian Genetic Algorithm used by Autodock, the ligand is defined as a chromosome that has seven standart genes accounting for the ligand's Cartesian coordinates (for the ligand translation) and four variables specifying its orientation. Additional genes representing flexible torsional angles can also be identified. After the

genes are defined, the genetic algorithm starts with creating a population of random individuals restricted within a user stated box (grid box) that also contains the protein. For each individual, three translation (x,y,z), four orientation, and torsional angle genes are assigned randomly (within extents of grid maps for x,y,z, between -180^0 and $+180^0$ for orientation and torsional angle). These gene values of these random individuals are then converted into a corresponding phenotype that allows the assessment of each individual's fitness (total interaction energy of the ligand) (Morris *et al.,* 1998). This process is followed by a selection procedure that decides which individuals will be allowed to reproduce and is based on the following equation:

$$n_o = \frac{f_w - f_i}{f_w - \langle f \rangle} \qquad f_w \neq \langle f \rangle \tag{3.12}$$

Here, n_o is the number of offspring to be assigned to the individual, f_i is the fitness of the individual, f_w is the fitness of the worst individual (individual with the highest energy) and $\langle f \rangle$ is the mean fitness of the population. According to these equations, individuals with lower energy than the mean will always have a larger numerator, since f_w will always be higher than both $\langle f \rangle$ and f_i (except for the case $f_w = f_i$). Thus, the lower energy conformations will be allowed to carry their genes into next generation. In the case of $f_w = f_i$, the population is assumed to be converged and docking is terminated (Morris *et al.,* 1998) .

After the selection of reproducing individuals, biological crossover and mutation events take place to create the next generation. In the crossover process, equivalent genes are swapped. For instance, a one point crossover between chromosome BA and ba end up with chromosomes Ba and bA. A random mutation occurs on the basis of a Cauchy distribution is utilized to generate mutations on genes that are selected randomly.

In the Lamarckian Genetic Algorithm (Lamarck, 1914), each generation is followed by local search that based on the energy phenotype of each resulting chromosome, with translational step sizes of 0.2 Å, orientational and torsional step sizes of 5^0. If obtained conformation has lower energy than its predecessor, local search is repeated until

encountering higher energy conformation. This process followed by reverse-transcription of the optimised phenotype back into the genome. On the other hand, Darwinian local search is based on a blind phenotypic jump that can be either confirmed or ignored according to the phenotypic fitness. Thus, Lamarckian Genetic Algorithm is more efficient compared to Monte Carlo simulated annealing and traditional genetic algorithm (Figure 3.2) (Morris *et al*., 1998)

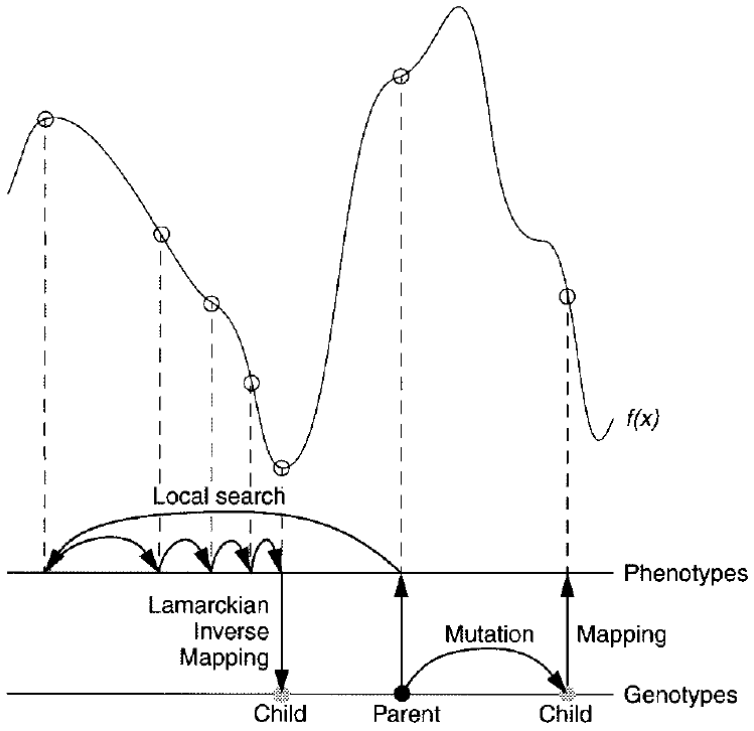

Figure 3.2. Darwinian(right) and Lamarckian(left) local search algorithms (Morris *et al*., 1998)

3.2.2. Scoring Function and Energy Evaluation in Autodock version 4.0

The force field in Autodock v4.0 evaluates binding in two steps which are shown in Figure 3.2. In the begining the ligand and protein start in an unbound conformation and the first step evaluates the intramolecular energetics of the transition state from unbound form to the bound form. In second step, when protein and ligand adopt in the bound complex, the intermolecular energetics of combining ligand and protein, are evaluated (Huey *et al*., 2007).

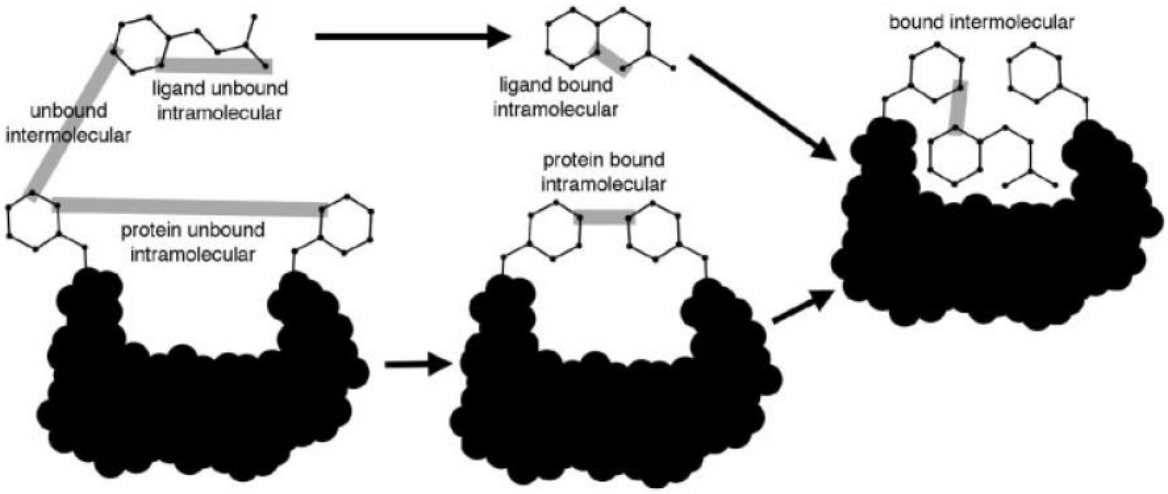

Figure 3.3. Energy evaluation of binding in Autodock v4.0 (Huey *et al*., 2007)

The force field includes six pair-wise evaluations ($\Delta G^{i\text{-}i}$) and an estimate of the conformational entropy lost upon binding (ΔS_{conf}):

$$\Delta G = (\Delta G_{bound}^{L-L} - \Delta G_{unbound}^{L-L}) + (\Delta G_{bound}^{P-P} - \Delta G_{unbound}^{P-P}) + (\Delta G_{bound}^{P-L} - \Delta G_{unbound}^{P-L} + \Delta S_{conf}) \quad (3.13)$$

In equation 3.11, L and P denotes for ligand and protein (receptor), respectively. (Huey at al., 2007). The two terms in the first paranthesis are intramolecular energies of bound and unbound states for ligand, respectively. The following two terms (in second paranthesis) are intramolecular energies of bound and unbound states for protein, respectively. The terms in third paranthesis represents the change in intermolecular energy between the bound and unbound states. $\Delta G_{unbound}^{P-L}$ is zero, since it is assumed that two molecules are adequately distant from one another.

The pair-wise terms (free energies, ΔG) in equation 3.12, is evaluated by a scoring function based on semiempirical free energy force field with the weighting constants (ΔG_i). These constants are experimentally determined by linear regression analysis from a set of protein-ligand complexes with known binding constants (Morris *et al.*, 1996, 1998). The Scoring function includes five terms to model dispersion/repulsion, hydrogen bonding, electrostatic interactions, internal ligand torsional constraints and desaolvation effects:

$$\begin{aligned}\Delta G = {} & \Delta G_{\mathrm{vdW}} \sum_{i,j} \left(\frac{A_{ij}}{r_{ij}^{12}} - \frac{B_{ij}}{r_{ij}^{6}} \right) \\ & + \Delta G_{\mathrm{hbond}} \sum_{i,j} E(t) \left(\frac{C_{ij}}{r_{ij}^{12}} - \frac{D_{ij}}{r_{ij}^{10}} \right) \\ & + \Delta G_{\mathrm{elec}} \sum_{i,j} \frac{q_i q_j}{\varepsilon(r_{ij}) r_{ij}} \\ & + \Delta G_{\mathrm{tor}} N_{\mathrm{tor}} \\ & + \Delta G_{\mathrm{sol}} \sum (S_i V_j + S_j V_i) \mathrm{e}^{(-r_{ij}^2/2\sigma^2)}\end{aligned} \tag{3.14}$$

Here, first term is a typical Lennard-Jones 6/12 potential for dispersion/repulsion interactions. Distance between the atoms i and j is represented by r_{ij}. A and B are Amber force field's parameters (Weiner *et al*., 1984). The second term is a directional H-bond term based on a 10/12 potential. E(t) is a directional weight that depends on the angle (t) between the probe and the target atom (Goodford, 1984). The third term represents the Coulomb potential for electrostatic interactions between charged particles. The parameters q_i, q_j are partial charges of the atoms, ε is the permittivity. Entropic penalty term is for the loss of torsional entropy upon binding (ΔG_{tor}), that is directly proportional to the number of rotatable bonds in the molecule (N_{tor}). The last term is a desolvation potential based on the volume (V_i and V_j) of the atoms surrounding a given atom. Parameter S (S_i and S_j) and σ are the weighting factors for volumes and distance, respectively (Stouten *et al.,* 1993).

In Autodock, energy calculations are performed by creating grid maps before starting the docking of the ligand to the receptor. These maps are calculated by Autogrid and created by placing the receptor protein inside a user defined three dimensional grid box. Probe atom is placed on each grid point, seperated by "grid spacing" and the maps are created for each type of atom involved in docking (C, O, N etc), then these maps are stored in seperate grid files that can later be sampled by the main auto-docking routine. Thus, recalculation of the distances involved in scoring function at each energy evaluation is avoided and this leads to a decrease in computational time (Morris *et al.,* 2001).

3.2.3. Methodology and Analysis of Docking Experiments

Blind docking methodology was applied in all docking experiments to investigate the selectivity of benzothiazoles for the interface region of TcTIM and hTIM. The target region was selected as the whole monomer structure for the monomer case, whereas one of the monomers and interface region were selected for the dimer cases, as illustrated in Figure 3.2. Protein was held rigid in all dockings, whereas ligand held flexible. Flexible torsional bonds during docking are indicated in Table 2.1. Flexibility of protein (both main and side chain) is included through different conformers.

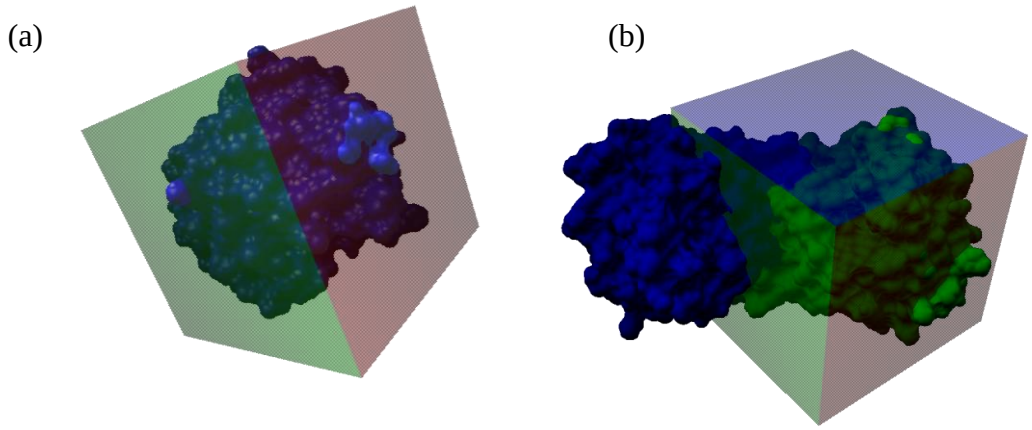

Figure 3.4. Grid box representation for (a) blind rigid monomer, (b) blind rigid dimer

The Lamarckian Genetic algorithm of Autodock v4.0 (Morris *et al.,* 2009) was used to explore the conformational space. 100 runs were perfomed for each docking experiment with each run consisting of $26x10^6$ energy evaluations. Grid boxes were constructed with a spacing of 0.375 Å with dimensions of 126 Å x 126 Å x 126 Å for all monomer and dimer dockings (Figure 3.3).

In the analysis part of docking experiments' results, the conformations were clustered according to the lowest energy conformation in each cluster. In order to analyze the binding modes, the highest ranking clusters within 1 kcal/mol of the lowest energy conformer were selected. The interactions and positions of the ligands in those conformers were visualized with Autodock GUI and 2D interaction diagrams that were obtained by using MOE software tool (Clark *et al*., 2006). Moreover, the residues within 4.5 Å distance to the ligand were determined for each cluster through the reports of MOE 2D interaction

diagrams. These reports were further utilized to detect the frequency of interaction of each residue with the ligand and a percentage value of occurence was calculated by using the following formula:

$$\%\ of\ \ occurrence = 100 \times \frac{number\ of\ \ occurrence\ of\ \ a\ residue\ within\ \ 4.5\ \text{Å}}{total\ \ number\ of\ \ conformations\ within\ 1\ kcal/mol} \quad (3.15)$$

These percentage of occurrence values were used to construct the percentage occurrence graphics and find out the specific binding regions of the ligands. All figures are drawn by PyMol v0.99 program (Delano, 2002).

3.2.4. Determination of Interface Residues

The residues that lie in the interface between the subunits (interface residues) were detected according to their SASA (Solvent Accessible Surface Area) differences between monomer and dimer forms (listed in Table 3.2) of TcTIM and hTIM. SASA values for both crystal structure and chosen conformers are calculated (M. Gerstein, 1992). 47 residues and 42 residues were determined as the interface residues for TcTIM and hTIM, respectively. These residues are listed in Appendix A.

4. RESULTS AND DISCUSSION

4.1 Blind TcTIM Monomer Dockings

Monomer dockings were carried out to investigate whether the TcTIM interface that opens up upon dissociation of the dimer presents any favorable binding site for benzothiazoles (Table 2.1) and especially for the inhibitors (ligands 8,9 and 10). As mentioned earlier two conformers that are M1 and M2 were chosen for monomer dockings and all highest ranking clusters that lie within 1 kcal/mol of the lowest energy conformation were analyzed for both two conformers (M1 and M2). To observe occurrence density of ligands on monomer, each residue was colored with respect to its percentage of occurrence value on monomer structure to form the percentage of occurrence figures (Figures 4.1 and 4.2). In these figures, the interface was showed as white meshed surface and colors indicated the percentage of occurrence value intervals, the color code runs approximately from blue (0-12 %), light blue (13-24%), cyan (25-36%), green (37-48%), yellow (49-60%), orange (61-72%) to red (73-84%).

The color coded percentage of occurrence value of each residue was shown in Figures 4.1 (for ligands 2 and 3) and 4.2 (for ligands 8, 9 and 10). As expected, the results show that the inhibitory ligands 8,9 and 10 select interface region more often compared to ligands 2 and 3 with no inhibitory effect. This difference between inhibitors and non-inhibitors can also be observed from the percentage of occurrence graphs in Figure 4.3. Ligands 8, 9 and 10 have higher occurence percentage of interface residues compared to ligand 2 and 3. Still the non-interface regions are more often selected by all five ligands (Figures 4.1 and 4.2). This suggests that the interface region on the monomeric state does not present the most preferred binding region for ligands. Lowest energy conformations at the interface for ligands 3, 8, 9 and 10 were also shown on M2 in Figure 4.4 (a-b). Here, ligand 9 is surrounded by interface residues at its most favorite binding pose on interface. However, ligands 3, 8 and 10 prefer a binding pose near to the interface residues. Ligand 2 does not select the interface region on M2.

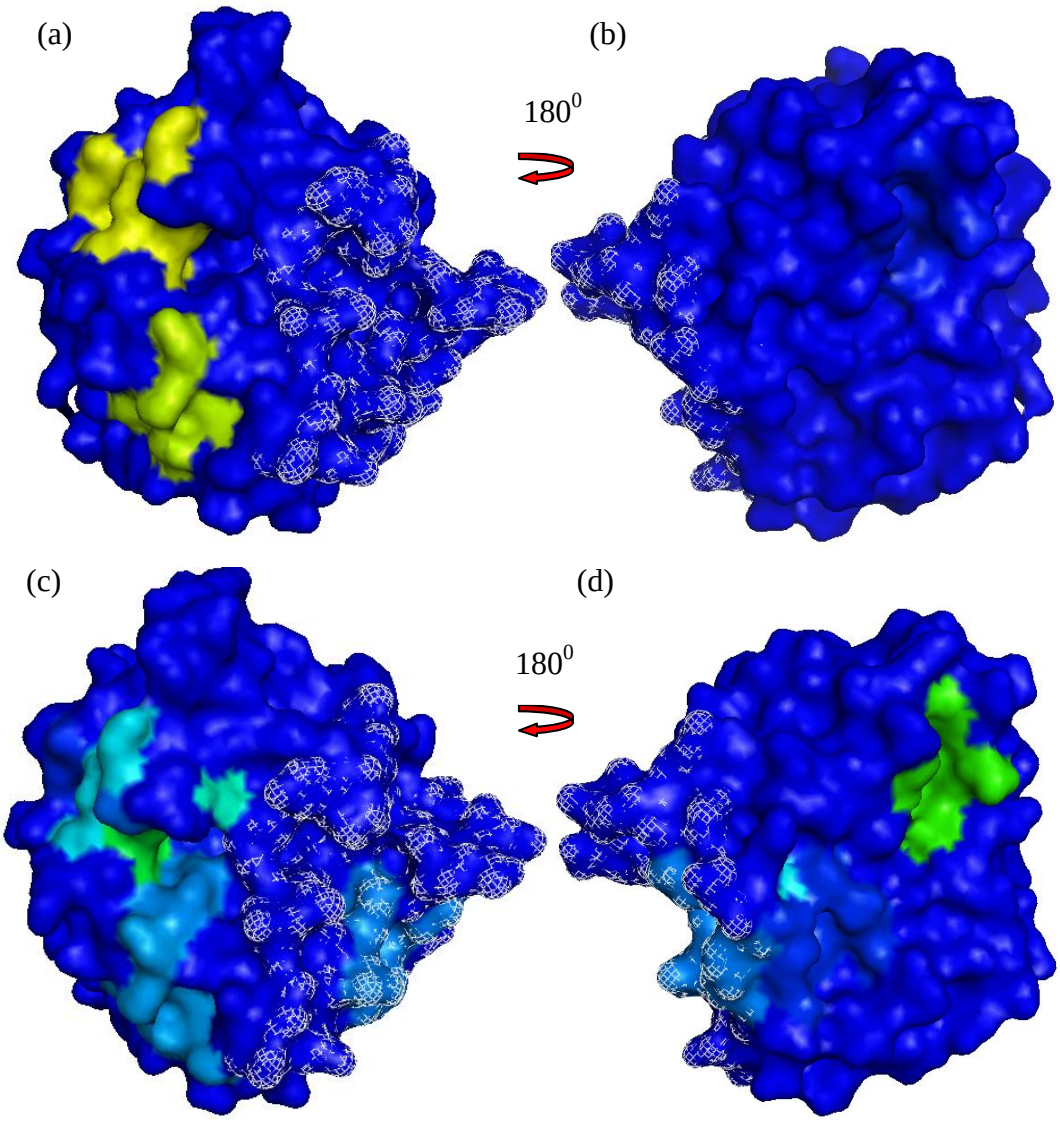

Figure 4.1. Occurrence density for TcTIM monomer conformers: (a-b) ligand 2, (c-d) ligand 3

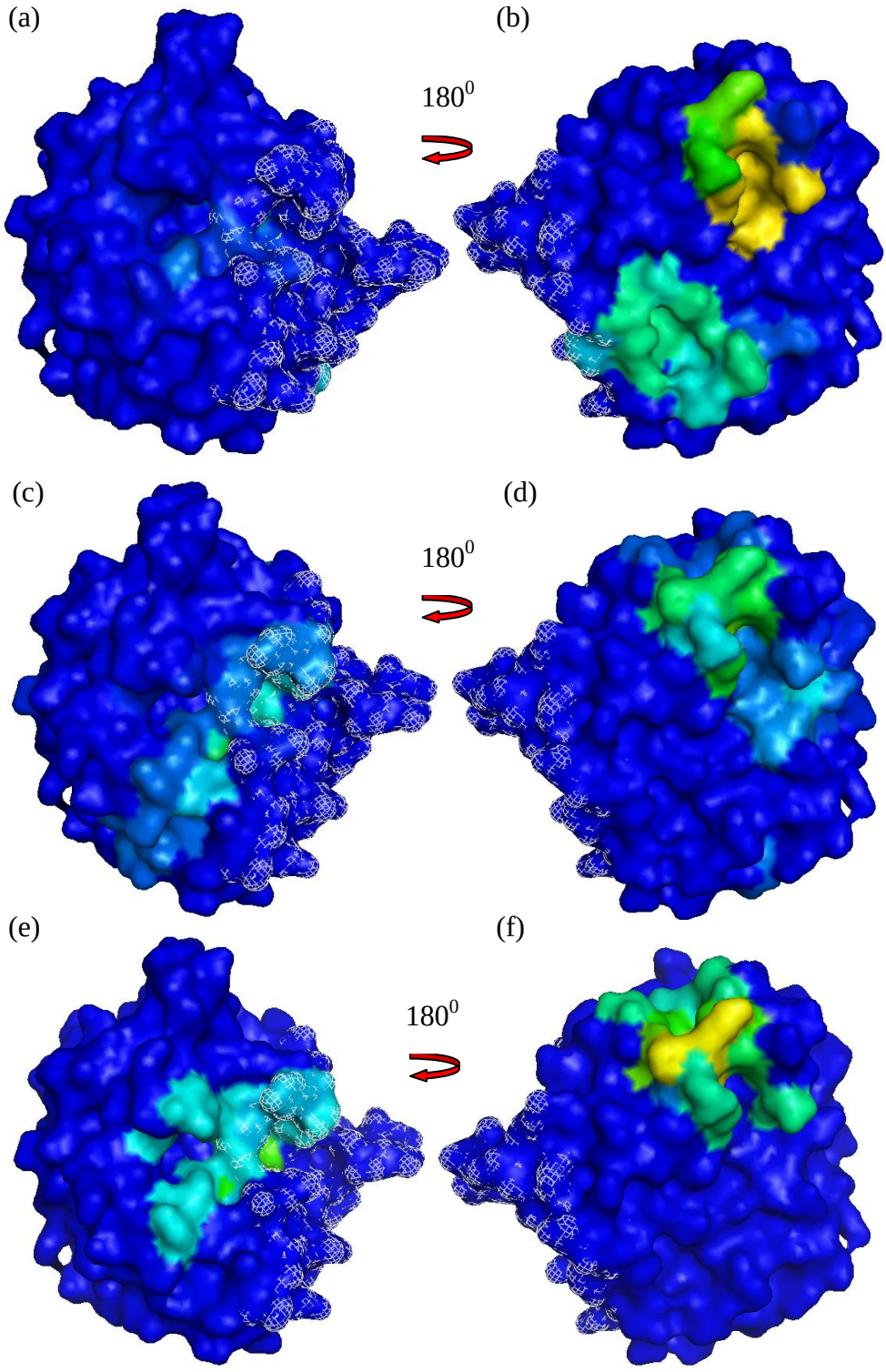

Figure 4.2. Occurrence density for TcTIM monomer conformers: (a-b) ligand 8, (c-d) ligand 9, (e-f) ligand 10

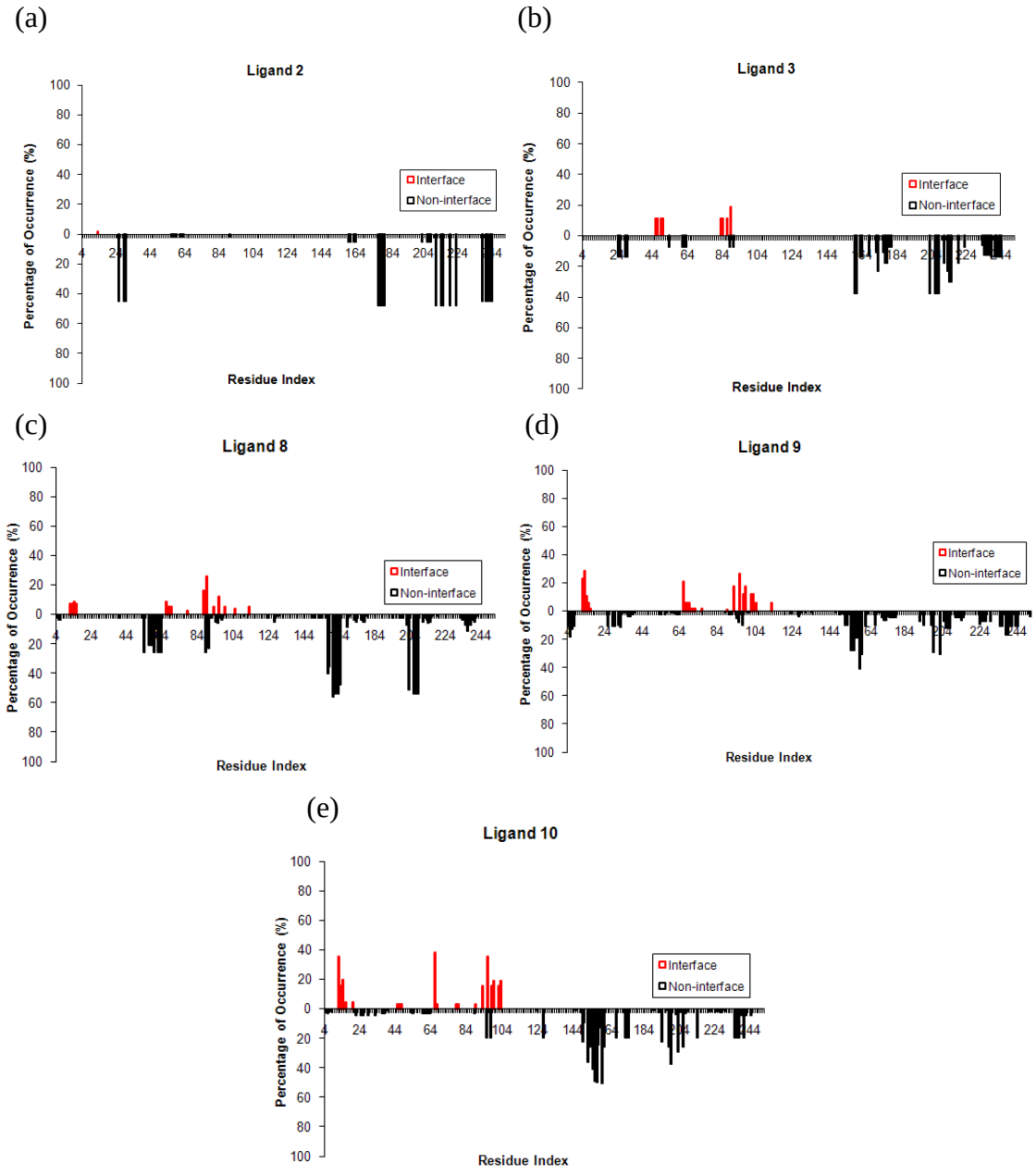

Figure 4.3. Percentage values of occurrence graphs for monomer residues at a distance of 4.5 Å to ligand, (a) ligand 2, (b) ligand 3, (c) ligand 8, (d) ligand 9, (e) ligand 10

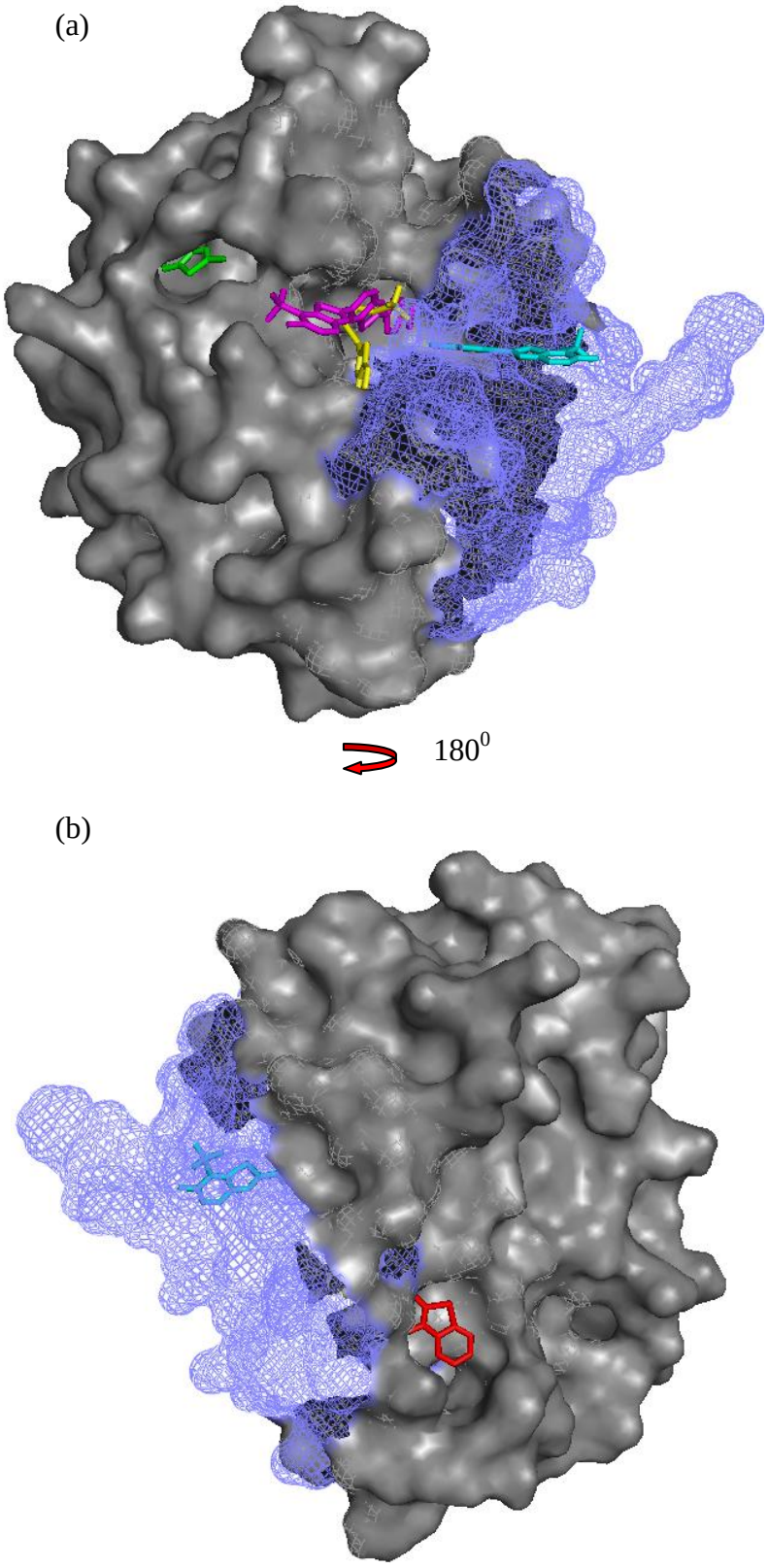

Figure 4.4. Lowest energy conformations at the interface of conformer M2 are given for (a) ligand 2 (green), ligand 8 (yellow), ligand 9 (cyan), ligand 10 (magenta) and (b) ligand 3 (red). Interface is the meshed purple region.

Table 4.1. Docking scores and the number of occurrences at the interface for TcTIM monomer dockings

Monomer Dockings	M1	M2	Fraction of Occurrence at interface
	ΔG (kcal/mol) (Cluster #)	ΔG (kcal/mol) (Cluster #)	
Ligand 2	-	-	0/200=0.00
Ligand 3	-	-4.75 (6th)	23/200=0.12
Ligand 8	-7.00 (4th)	-6.93 (1st)	24/82=0.29
Ligand 9	-6.29 (3rd)	-6.38 (1st)	53/185=0.29
Ligand 10	-7.56 (2nd)	-7.22 (4th)	61/159=0.38

Lowest free energy of binding for ligands at the interface are listed in the Table 4.1. ΔG is the estimated free energy of binding in AutoDock, which is also used as a score. Reported ΔG values belong to the lowest energy conformation at the interface. Fraction of occurrence at interface is calculated from the ratio of number of conformations at the interface over the number of conformations within 1kcal/mol based on the lowest energy conformation. The conformations, in which at least two interface residues fall within 4.5 Å distance of the ligand, are labeled as "conformations at the interface". Ligand 2 has no conformation at the interface and ligand 3 only chooses interface at the 6th cluster on M2. On the other hand, ligands 8, 9 and 10 bind to the interface at lower energy clusters. The free energy of binding values indicate that inhibitory ligands also show higher affinity for the receptor. Especially, in the case of ligand 10, the free energy of binding values are lower than other ligands' energy values. The extra aromatic group in the structure of ligand 10 may be related with lower free energy of binding values, since this extra aromatic group may form π-π and cation-π interactions with the residues around the ligand (Figure 4.5 (e-f)). The ratios for the selection of interface (last column in Table 4.1) by the ligands verify that the inhibitors more often prefer binding to the interface region than non-inhibitors.

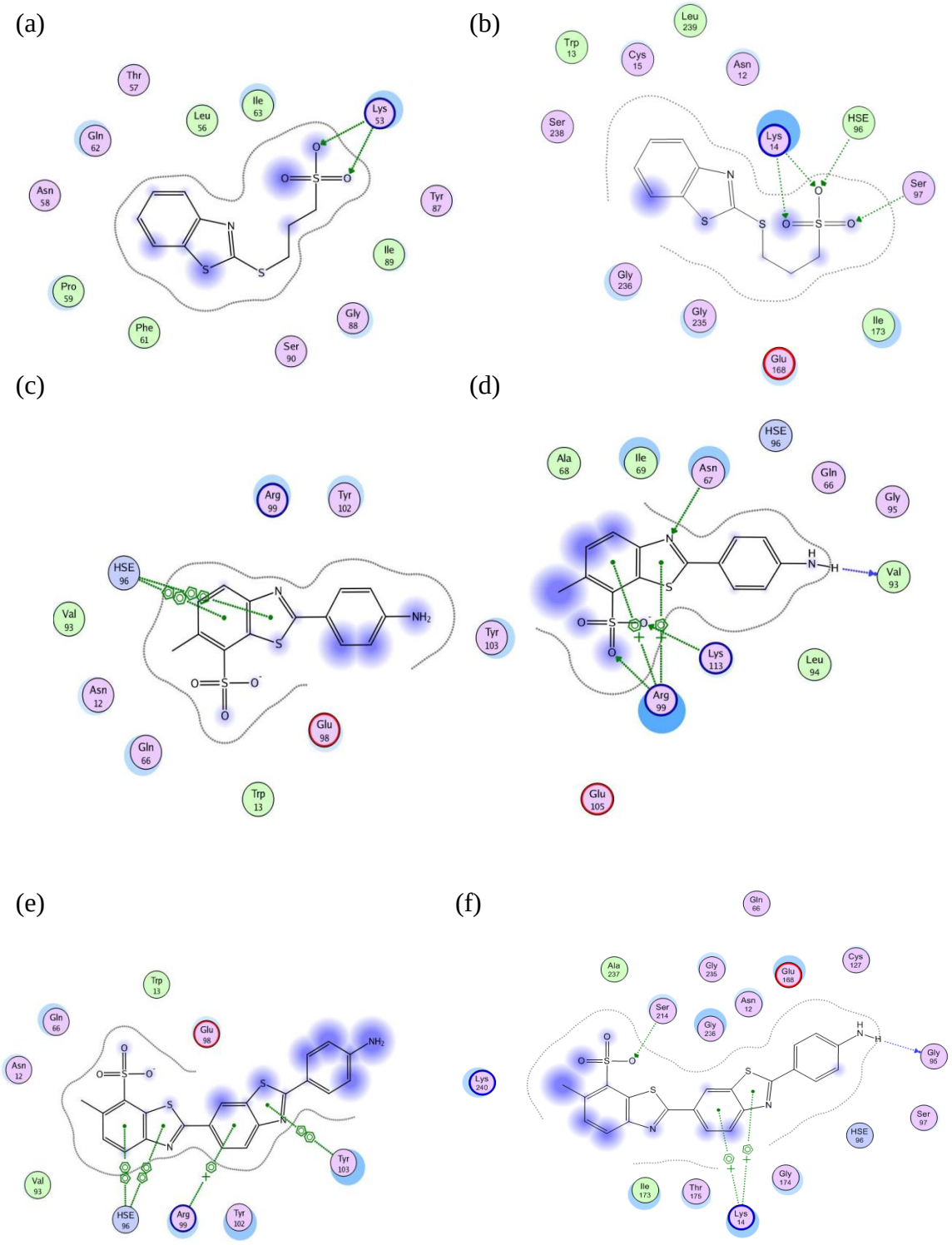

Figure 4.5. TcTIM monomer dockings: MOE 2D diagrams indicating the interactions between ligands 8 (a-b), 9 (c-d), 10 (e-f) at lowest energy conformations on the interface. The figures on the left are for M1 and on the right for M2.

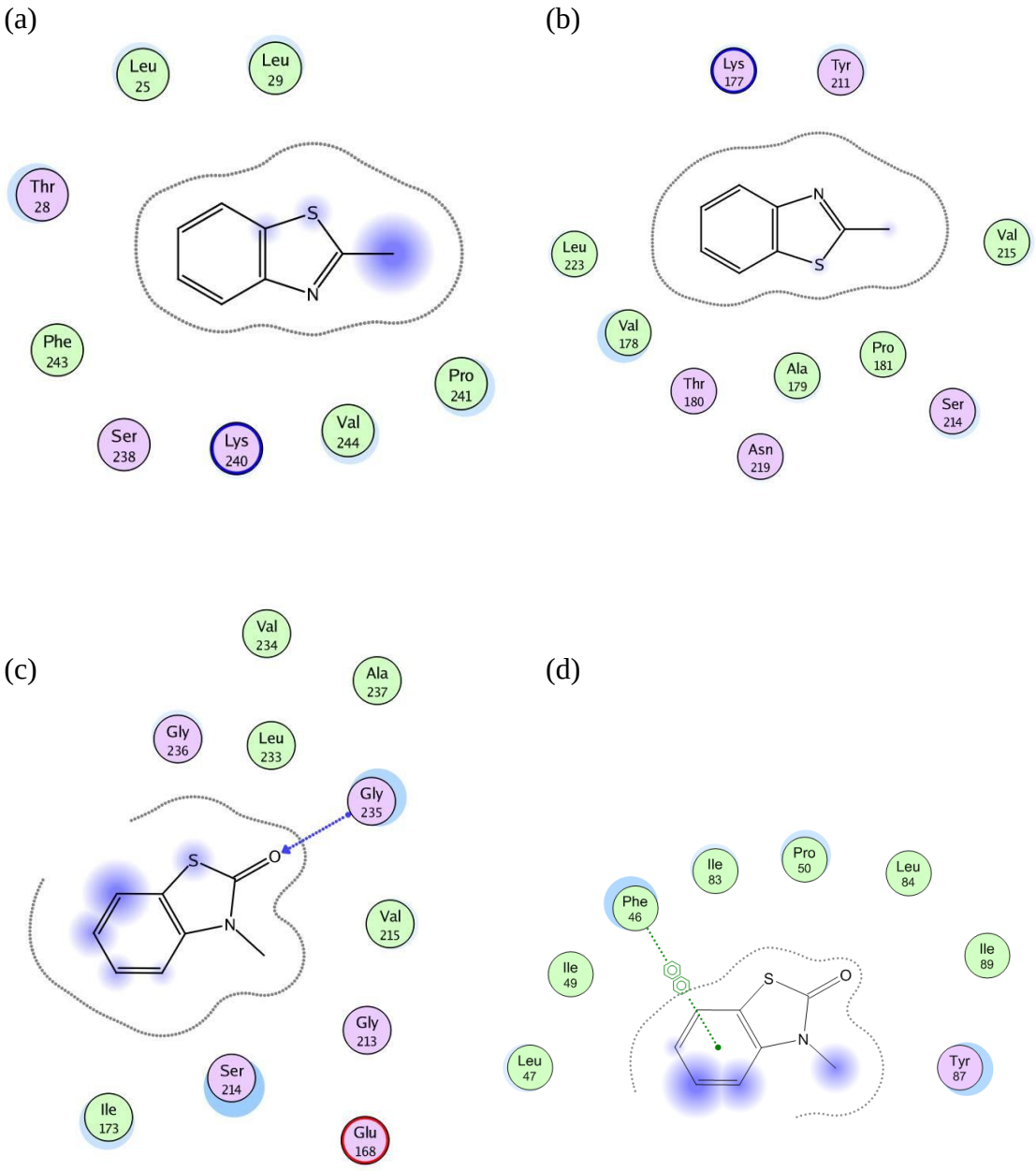

Figure 4.6. TcTIM monomer dockings: MOE 2D diagrams indicating the interactions between ligands 2 (a-b), 3 (c-d). The figures on the left are for M1 and on the right for M2.

In the Figure 4.5, the MOE diagrams are given for the high scoring conformations in which the interface is selected by ligands 8, 9 and 10. These MOE 2D diagrams indicate the interactions between ligands and surrounding residues within 4.5 Å. The ligands with inhibitory effect make specific interactions with the interface residues. For instance, ligand 8 makes H-bonding with Lys14, His96 (catalytic residues) and Lys113. H-bonding is also observed between sulfonate group of ligand 9 and Arg99, Lys113, nitrogen of ligand 9's benzothiazole group and Asn67. Moreover, there are aromatic interactions between ligands 9, 10 and interface residues; π-π interactions are observed between ligand 9 and His 96, ligand10 and His96, Tyr103 in the lowest energy conformations at the interface. There are also cation-π interactions between ligand 9 and Arg99, ligand 10 and Lys14, Arg99. Figure 4.6 (a-b-c) show the interactions for the lowest energy conformations of ligand 2 and 3, Figure 4.6 (d) indicates the interactions of ligand 3 at the lowest energy conformation on the interface region of M2. In contrast to inhibitory ligands, ligand 2 does not make specific interactions with the interface residues. Ligand 3 makes H-bonding with Gly235 in the lowest energy conformation on M2 (Figure 4.6 (c)) and π-π interaction with Phe46 in the lowest energy conformation at the interface on M2 (Figure 4.6 (d)).

To sum up, the results of the monomer dockings imply that inhibitors have selectivity for the interface region. However, the interface region of the monomeric form is not the primary binding site for the inhibitory ligands, since the ratios for selection of interface are not very high.

4.2 Blind TcTIM Dimer Dockings

In blind dimer dockings, the grid box covers an entire monomer and the interface region in order to investigate the inhibitory and non-inhibitory ligands' tendency to select the interface region between two subunits. The analysis for the blind rigid dockings was carried out for the conformations that lie within the 1 kcal/mol of the lowest energy conformation for D1,D2 and D3 conformers of TcTIM.

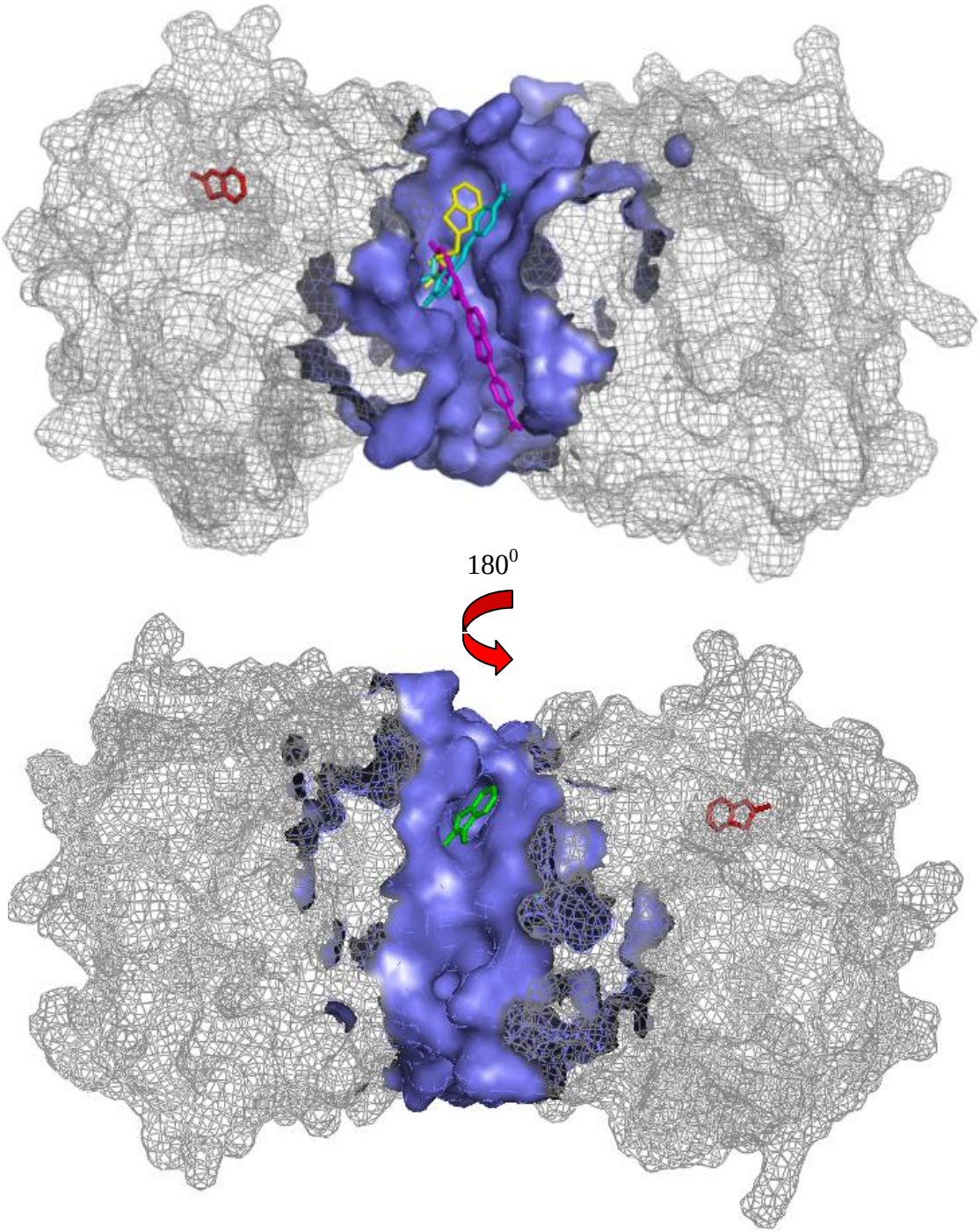

Figure 4.7. TcTIM dimer dockings: Lowest energy conformations for D1. The interface region is shown as “surface” (color: purple) together with ligand 2 (red), ligand 3 (green), ligand 8 (yellow), ligand 9 (cyan) and ligand 10 (magenta)

(a)

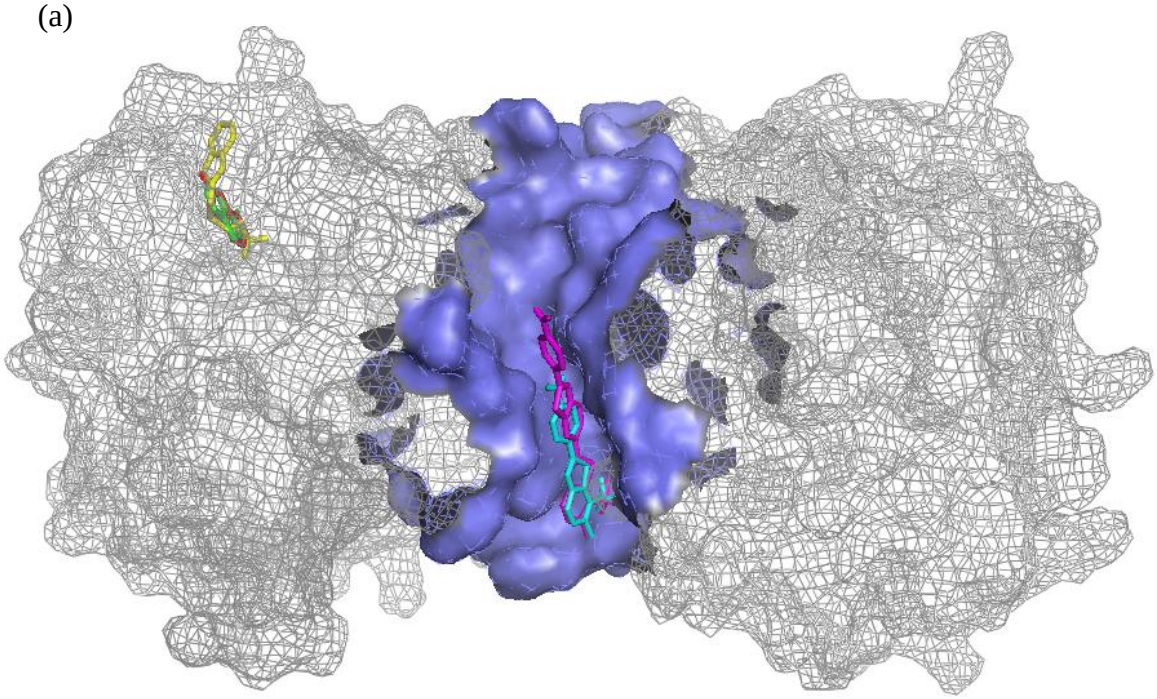

(b)

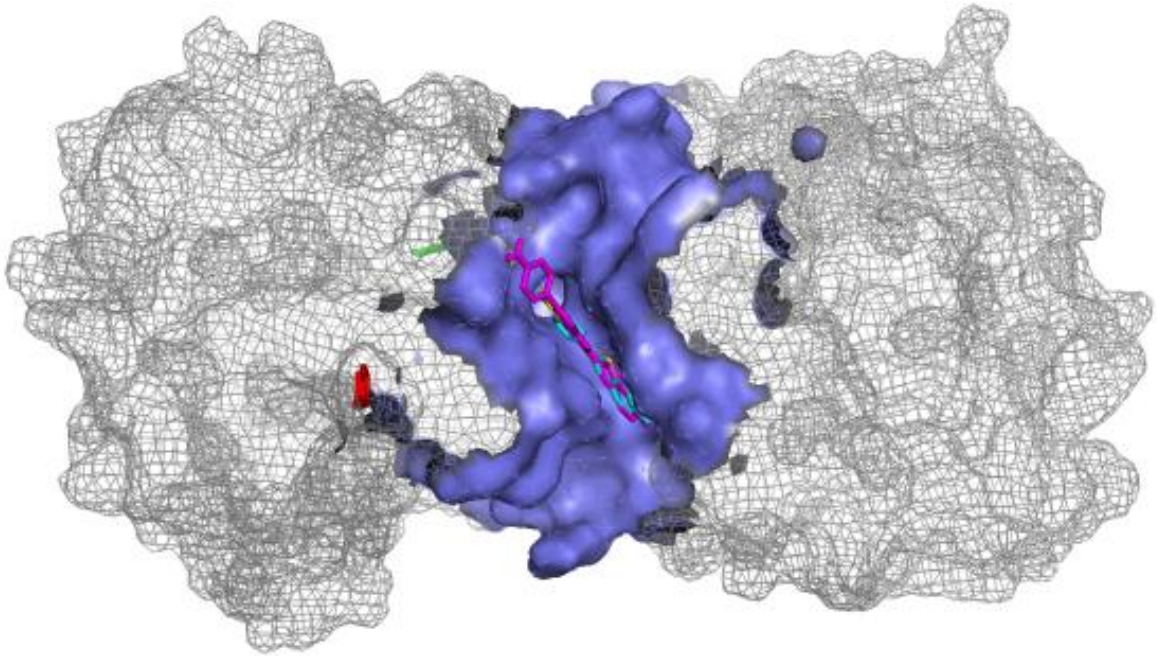

Figure 4.8. TcTIM dimer dockings: Lowest energy conformations for (a) D2 and (b) D3. The interface region is shown as “surface” (color: purple) together with ligand 2 (red), ligand 3 (green), ligand 8 (yellow), ligand 9 (cyan) and ligand 10 (magenta)

Figures 4.7 and 4.8, exhibits the lowest energy conformations of ligands on D1, D2, D3. The inhibitory ligands 8 (except D2), 9, 10 prefer to bind to the tunnel shaped cavity formed by residues of loop 3 (Ala68-Ser80) and residues Asn67, Arg99, Tyr102-Thr106, Lys113 on the interface region. Non- inhibitory ligands select the non-interface region, except ligand 3 on D1. However, ligand 3 does not bind to the tunnel shaped cavity in that conformation. Moreover, the inhibitory ligands tend to lie in a planar position in the tunnel region, along the cavity of interface.

Figures 4.9 and 4.10 are occurrence density figures (that show percentage of occurrence values of residues) in which the color code runs approximately from blue (0-12 %), light blue (13-24%), cyan (25-36%), green (37-48%), yellow (49-60%), orange (61-72%) to red (73-84%). The results show that, inhibitory ligands (ligands 8,9 and 10) have higher percentage values of occurence for interface residues compared to non-inhibitory ligands (ligands 2 and 3).Therefore, ligands 8, 9 and 10 preferentially bind to the interface. On the other hand, ligands 2 and 3 generally prefer to bind the cavities away from interface (Figure 4.9 (a), (b), and (d)). Selection of the interface region is dominantly observed for ligands 9 and 10 with very high percentage of occurence for interface residues (Figures 4.9 (g) and (i), 4.10 (d) and (e)). These residues are Ile69, Arg99, Tyr103, Glu105,and Lys113 for ligand 9, Ile69, Arg99, Tyr102, Tyr103, Gly104, Glu105, and Lys113 for ligand 10. Especially, ligand 10 shows the highest specificity besides affinity compared to ligand 8 and 9. This result is also consistent with the lower IC50 value of ligand 10 (Table 2.2) (Tellez-Valencia *et al.,* 2002). Figures 4.11, 4.12 and 4.13 show the interactions between inhibitors (ligands 8, 9 and 10 respectively) and TcTIM conformers. Ligands 8,9 and 10 make H-bonding especially with residues Asn67,Arg99 and Lys113 in the lowest energy conformations on conformers D1 and D3. Specifically, the sulfonate group makes multiple H-bonds, which can contribute to the stability of the enzyme-ligand complex. Thus, the sulfonate group of inhibitors may a have role not only in the dissolution of the ligands, as stated in previous works (Espinoza-Fonseca and Trujilo-Ferrara, 2004) but also in the specificity and the binding affinity of the inhibitors. To investigate this issue, blind dockings with derivatives of ligands 2, 8, 9, and 10 (either with added or deleted sulfonate) were also performed on D3 conformer. The results will be discussed under the part called "TcTIM Dimer Dockings with Derivatives of Ligands". Moreover, Ligands 9 and 10 make H-bonding with Thr70 and π-π interactions with Tyr103 on the conformer D2.

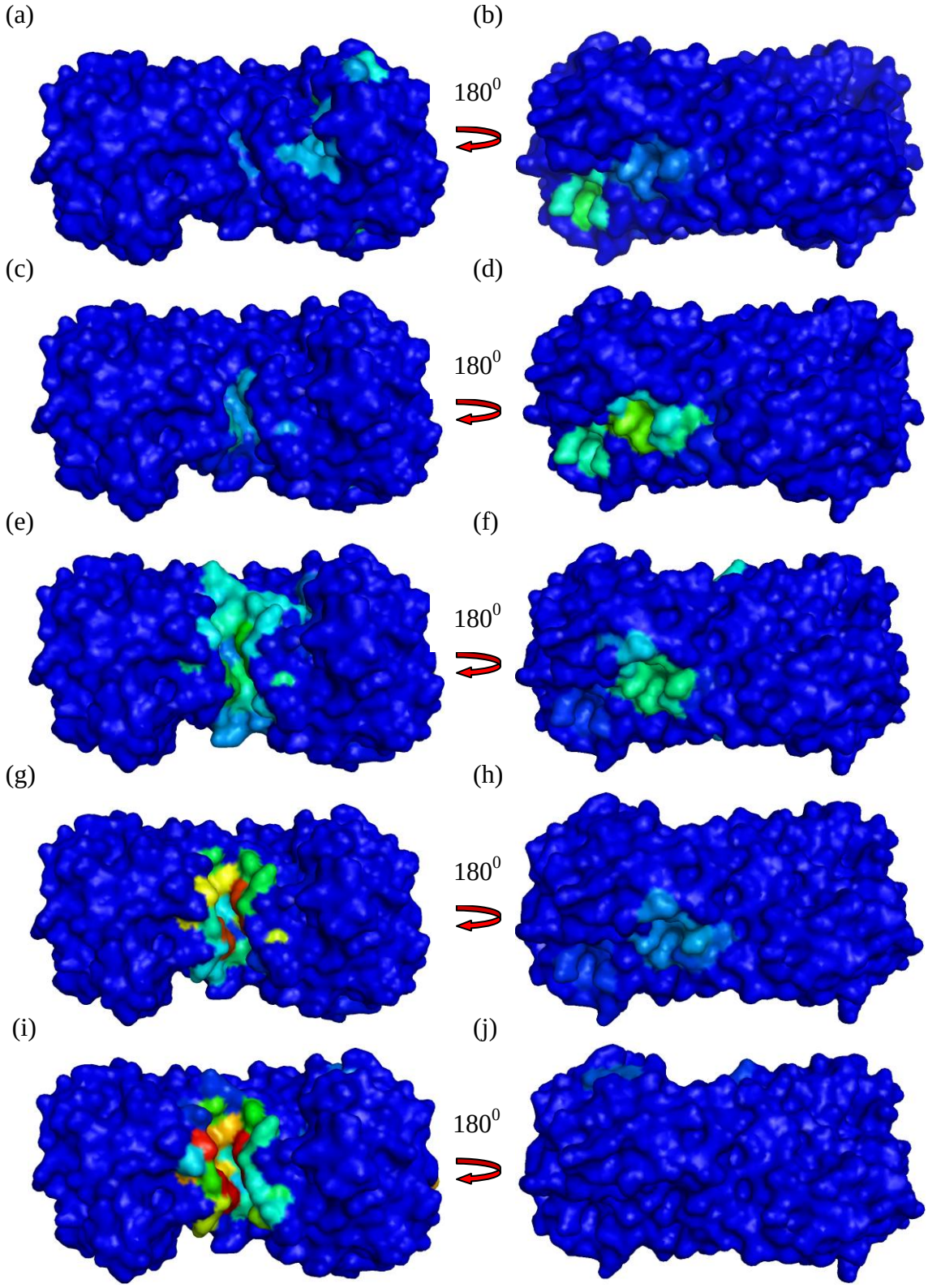

Figure 4.9. Occurrence density values for TcTIM dimer conformers: (a-b) ligand 2, (c-d) ligand 3, (e-f) ligand 8, (g-h) ligand 9, (i-j) ligand 10

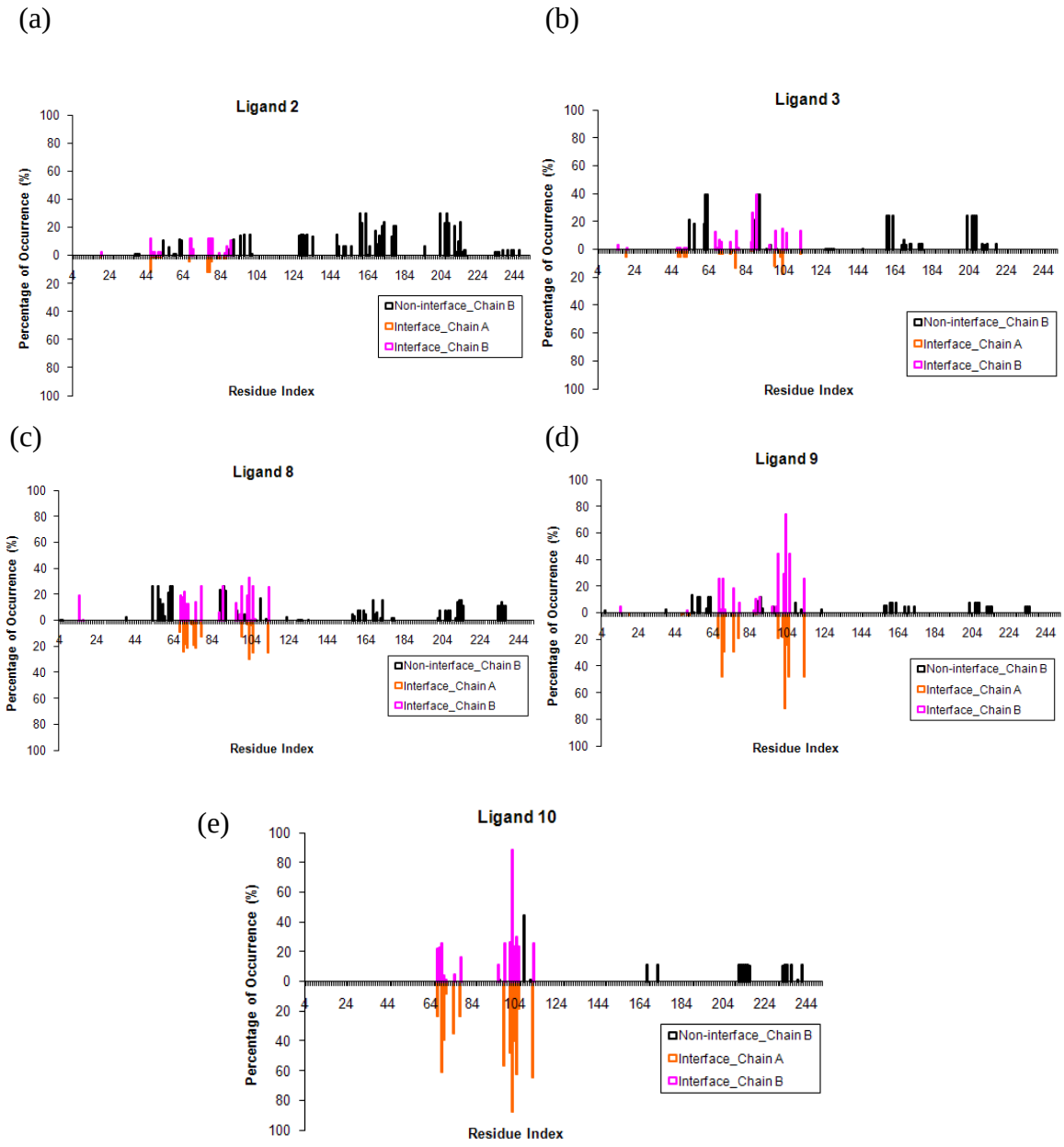

Figure 4.10. Percentage values of occurrence graphs for TcTIM dimer residues at a distance of 4.5 Å to ligand, (a) ligand 2, (b) ligand 3, (c) ligand 8, (d) ligand 9, (e) ligand 10

(a)

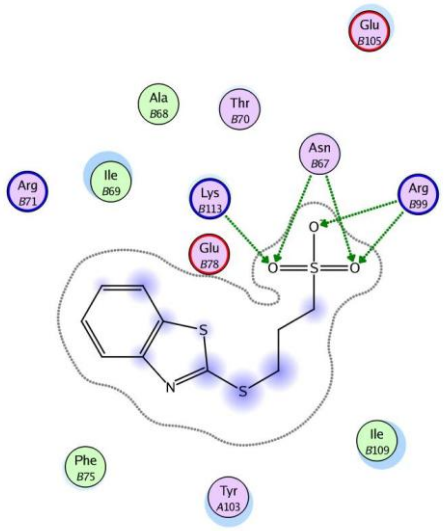

(b)

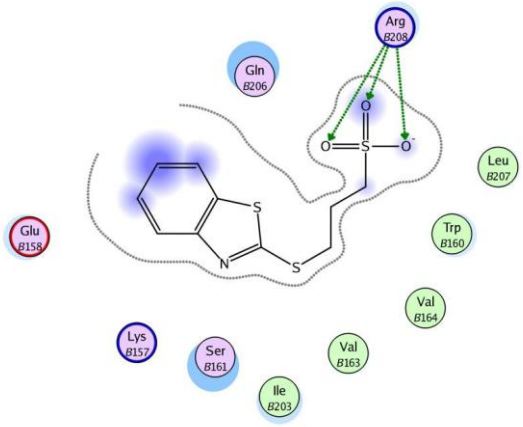

(c)

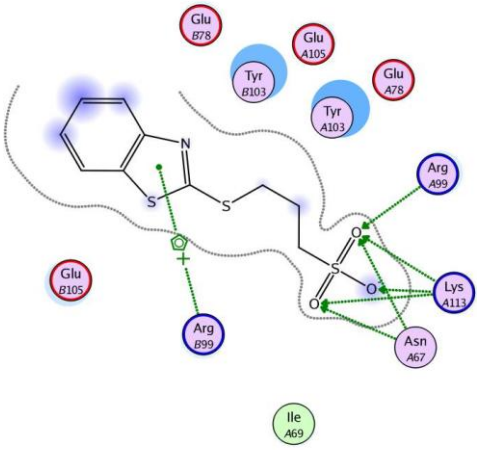

Figure 4.11. TcTIM dimer dockings: MOE 2D diagrams indicating the interactions between ligand 8 and surrounding residues within 4.5 Å at the lowest energy conformations. (a) D1-ligand 8, (b) D2-ligand 8, (c) D3-ligand 8

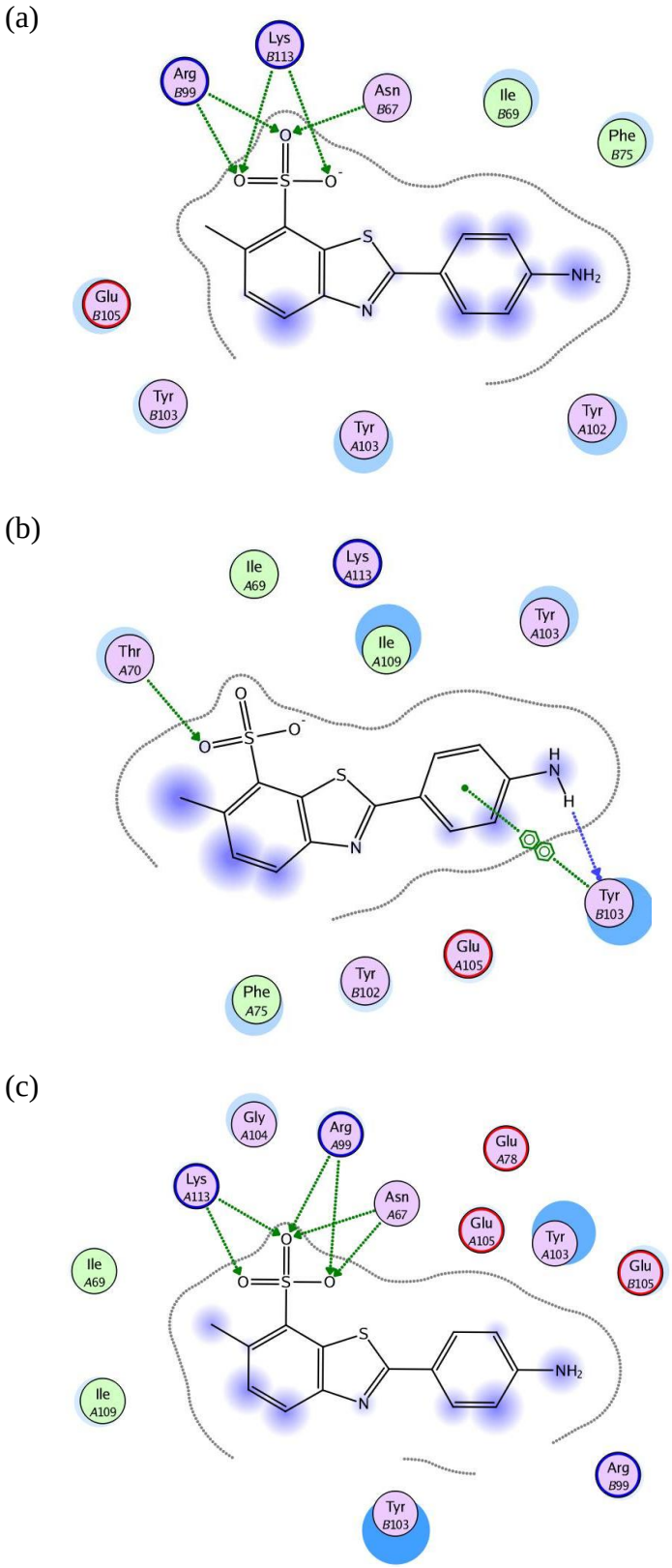

Figure 4.12. TcTIM dimer dockings: MOE 2D diagrams indicating the interactions between ligand 9 and surrounding residues within 4.5 Å at the lowest energy conformations.(a) D1-ligand 9, (b) D2-ligand 9, (c) D3-ligand 9

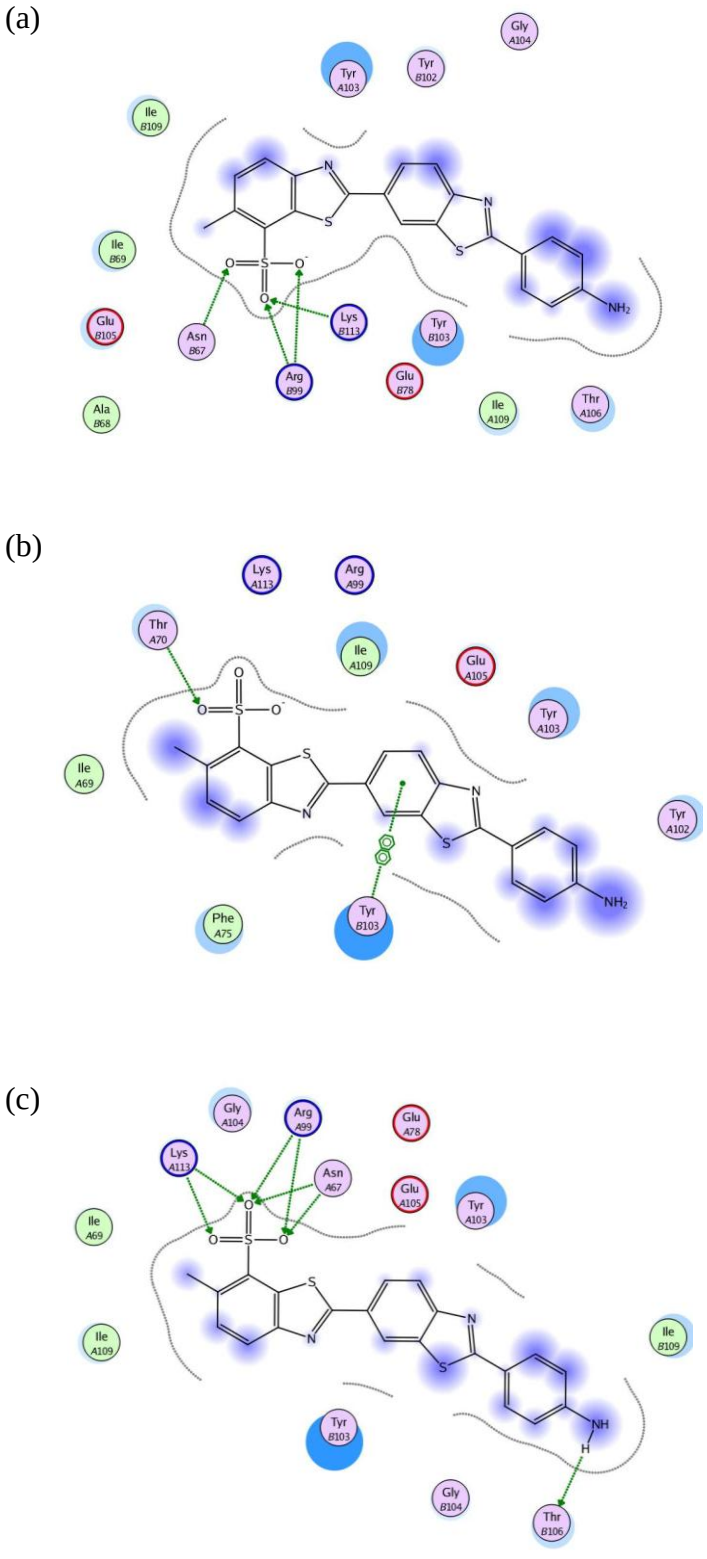

Figure 4.13. TcTIM dimer dockings: MOE 2D diagrams indicating the interactions between ligand 10 and surrounding residues within 4.5 Å at the lowest energy conformations. (a) D1-ligand 10, (b) D2-ligand 10, (c) D3-ligand 10

Table 4.2. Docking scores and the number of occurrences at the interface for TcTIM dimer dockings

Dimer Dockings	D1	D2	D3	Fraction of Occurrence at interface
	ΔG (kcal/mol) (Cluster #)	ΔG (kcal/mol) (Cluster #)	ΔG (kcal/mol) (Cluster #)	
Ligand 2	-4.64 (3rd)	-5.06 (3rd)	-4.55 (3rd)	47/300=0.16
Ligand 3	- 4.83 (1st)	-	-4.80 (1st)	139/300=0.46
Ligand 8	- 6.67 (1st)	-6.61 (5th)	-7.10 (1st)	150/202=0.74
Ligand 9	- 7.10 (1st)	-6.89 (1st)	-7.67 (1st)	228/255=0.89
Ligand 10	- 8.38 (1st)	-8.90 (1st)	-9.27 (1st)	219/247=0.89

Lowest free energy of binding for ligands at the interface are listed in the Table 4.2. Ligands 8,9 and 10 choose the interface region in 74%, 89% and 89% respectively. These ratios are 16% and 46% for non-inhibitory ligands 2 and 3 (Table 4.2-last column). Inhibitory ligands prefer binding the interface in their lowest energy conformations (except ligand8-D2 complex). On the other hand, ligand 3 also selects the interface in its lowest energy conformations on D1 and D3. However, its binding poses on interface are different than inhibitory ligands. Ligand 3 binds away from tunnel shaped cavity as seen in Figure 4.7. In addition, the estimated free energy of binding values are appreciably lower for ligands 8,9 and 10 compared to non-inhibitory ligands due to the strong interactions like H-bonds, π-π and cation-π interactions (Figures 4.11, 4.12 and 4.13) between inhibitory ligands and the enzyme. Thus, the natural stability of interface may be disrupted by these interactions leading to inhibition. However, the actual mechanism of this process is not known currently.

The results of TcTIM dimer dockings suggest that the tunnel shaped cavity on the interface region of the dimer presents a more favorable binding site for the inhibitory ligands than the interface region of the monomeric form. This fact can be clearly observed by a comparison of data in Tables 4.1 and 4.2. Inhibitors select the interface region with 29-38% in the monomeric state, 74-89% in the dimeric state. Hence, it is most likely that

the inhibitory ligands bind to the enzyme during the dissociation of the monomers rather than their association.

4.3 Blind TcTIM Dimer Dockings with Derivatives of Ligands

In previous studies, it is claimed that sulfonate group is important for dissolvation of benzothiazoles (Espinoza-Fonseca and Trujilo-Ferrara, 2004). However, TcTIM dimer results show that sulfonate group of ligands 8, 9 and 10 makes multiple H-bonding predominantly with the interface residues Asn67, Arg99 and Lys113. To observe the role of the sulfonate group on the binding affinity and selectivity for the interface region, derivatives of ligands 2, 8, 9 and 10 (listed in Table 4.3) were created using CORINA web server (Sadowski *et al*., 1994). A sulfonate group was added to ligand 2 (i.e. it became 2-methylbenzothiazole-7-sulfonic acid), and the sulfonate group was removed from ligands 8, 9 and 10. Derivatives were docked to D3 conformer using the same blind docking methodology.

Table 4.3. Structure of Derivatives

Derivatives of Ligands	Structure
Ligand 2	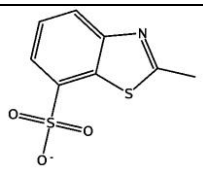
Ligand 8	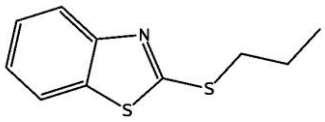
Ligand 9	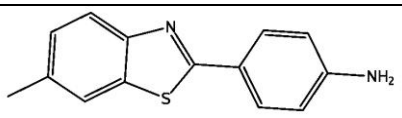
Ligand 10	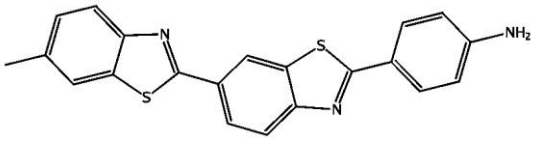

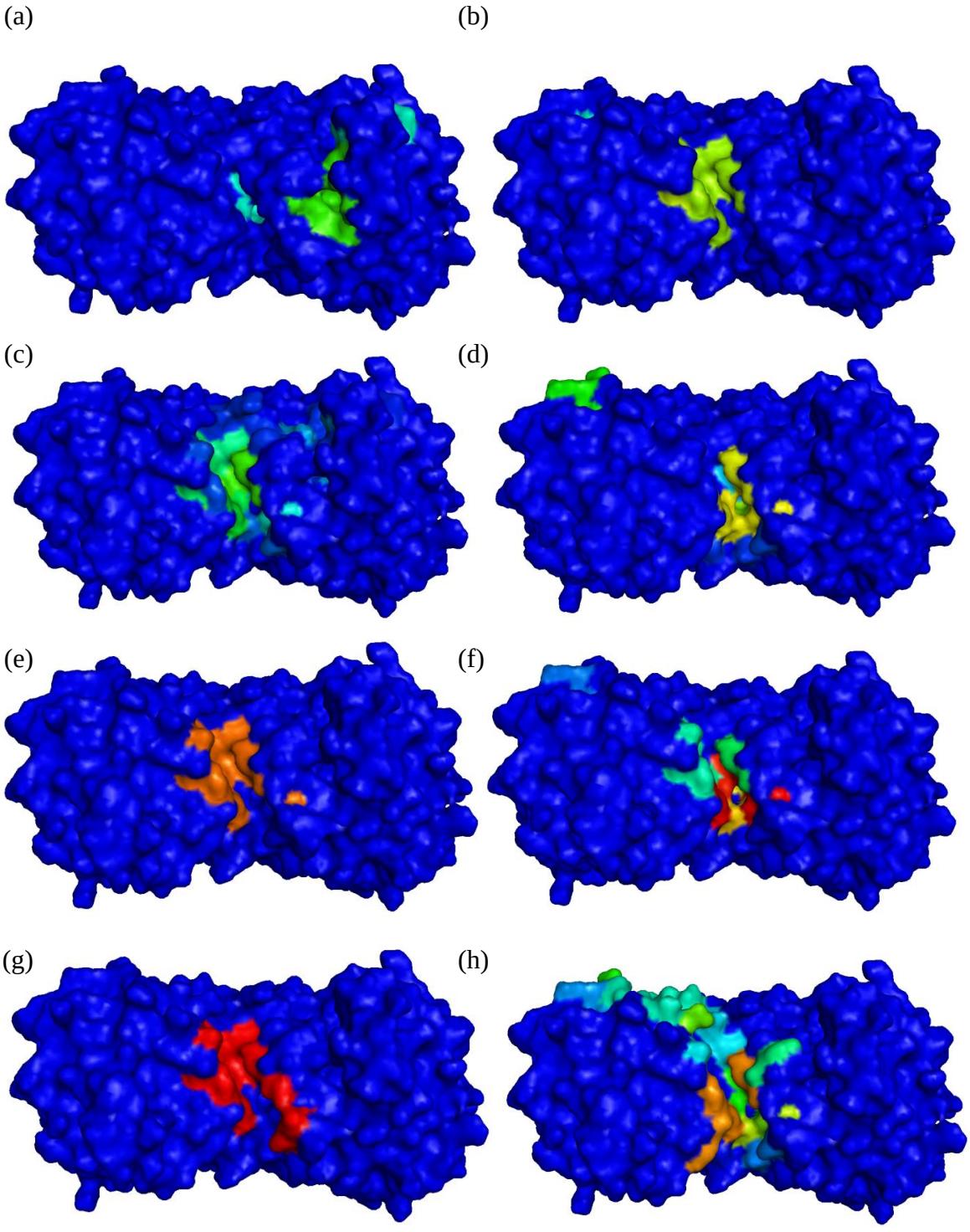

Figure 4.14. Occurrence density for benzothiazoles (ligands 2, 8, 9 and 10-left) and their derivatives (right) on D3 conformer of TcTIM dimer.

(a) (b) (c)

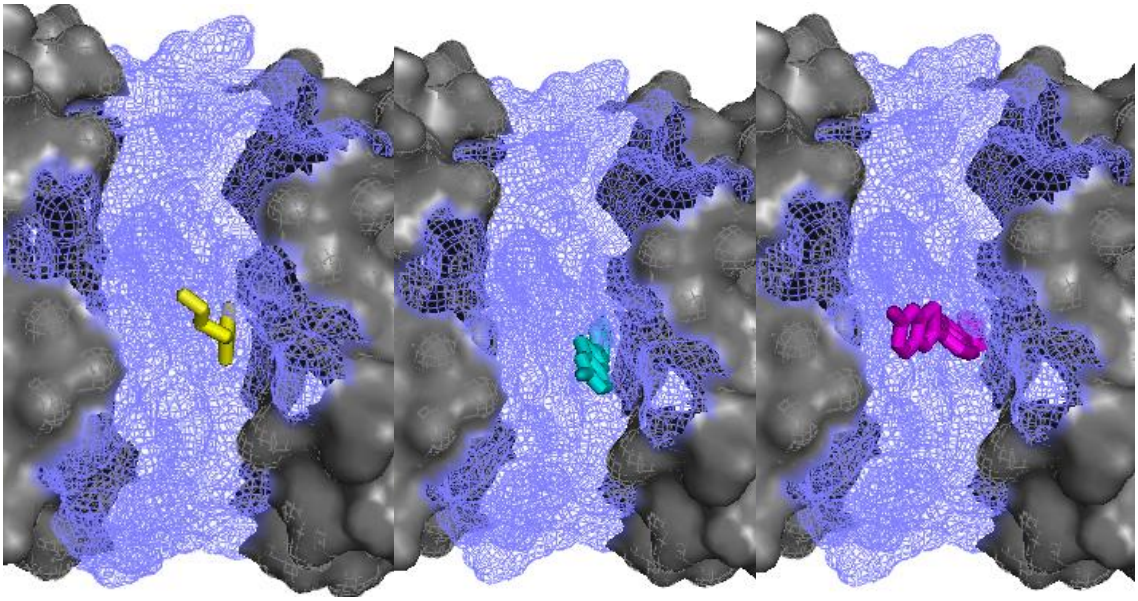

Figure 4.15. Perpendicular binding orientation of derivatives on D3 conformer: The interface region is shown as "meshed" (color: purple). (a) ligand 8 (yellow), (b) ligand 9 (cyan) and (c) ligand 10 (magenta)

The occurrence percentages of residues around the ligands docked to conformer D3, were used to construct Figure 4.14 and the color code runs approximately from blue (0-12 %), light blue (13-24%), cyan (25-36%), green (37-48%), yellow (49-60%), orange (61-72%) to red (73-84%). As explained in the previous section on TcTIM dimer dockings, ligand 2 is able to bind to various regions on the dimer (Figure 4.9 (a) and 4.10 (a)). However, addition of a sulfonate group to ligand 2 increases its selectivity for the interface region, as shown in Figure 4.14 (b). Deletion of sulfonate group from ligand 10 decreases the selectivity for the tunnel region of the interface (Figure 4.14 (g) and (h)). Although high occurrence percentages are present for the interface residues, derivatives of ligands 8 and 9 do not pursuit the binding pattern observed for original ligands 8 and 9. As seen in Figures 4.7 and 4.8, ligands 8, 9 and 10 lie along the tunnel shaped cavity on the interfae. In contrast, the majority (82%, 59%, %55 for ligands 8, 9 and 10 respectively) of the conformations at the interface, the derivatives of these ligands bind in a perpendicular manner to the interface region as seen in Figure 4.15. Thus, the absence of sulfonate group either decreases the selectivity for the interface region (ligands 2 and 10 cases) or changes the binding mode of the ligands (ligands 8, 9 and 10 cases).

Addition or deletion of sulfonate does not only change the binding poses of ligands, but also it affects the interactions with the enzyme. Figure 4.16 (a-b-c-d) show the MOE 2D diagrams that indicate the interactions between derivatives of ligands 2, 8, 9, 10 and surrounding residues within 4.5 Å at the lowest energy conformations. Figure 4.16 (e-f) represent the interactions between derivatives of ligands 8, 9 and the residues within 4.5 Å at the lowest energy conformations on the interface. The comparison between Figure 4.16 and Figures 4.11 (c), 4.12 (c), 4.13 (c) reveals that the derivatives of ligands 8, 9 and 10 don't tend to make H-bonding with the enzyme as much as original ligands, even if they bind to the interface region. For instance, ligand 9 makes H-bonding with the residues Gly72, Lys113 and ligand 10 only makes H-bonding with Asn67. However, ligands 9 and 10 make more H-bonding with the enzyme via their sulfonate group in their original form docked on D3 conformer. Furthermore, sulfonate group of the derivative ligand 2 makes H-bonding with Arg208, whereas original ligand 2 makes no interactions in the lowest energy conformation on D3. These results clearly indicate that the presence of sulfonate group is critical for positioning of the ligands in the tunnel via specific H-bonding besides the aromatic interactions.

Table 4.4. Free energy of binding, ΔG, of ligands and its derivatives for TcTIM dimer (D3) dockings

	LOWEST ENERGY (kcal/mol)	
	Original ligands on D3	Derivatives on D3
Ligand 2	-5.20	-6.17
Ligand 8	-7.10	-5.72
Ligand 9	-7.67	-6.11
Ligand 10	-9.27	-7.19

The estimated free energies of binding for the highest scoring conformations are appreciably lower for the ligands with sulfonate groups than for sulfonate-free ligands, as shown in Table 4.4. This suggests that, ligands with sulfonate group form more stable ligand-enzyme complexes than sulfonate-free ligands and the presence of sulfonate group in the structure adds more stability to complexes through molecular interactions with the enzyme.

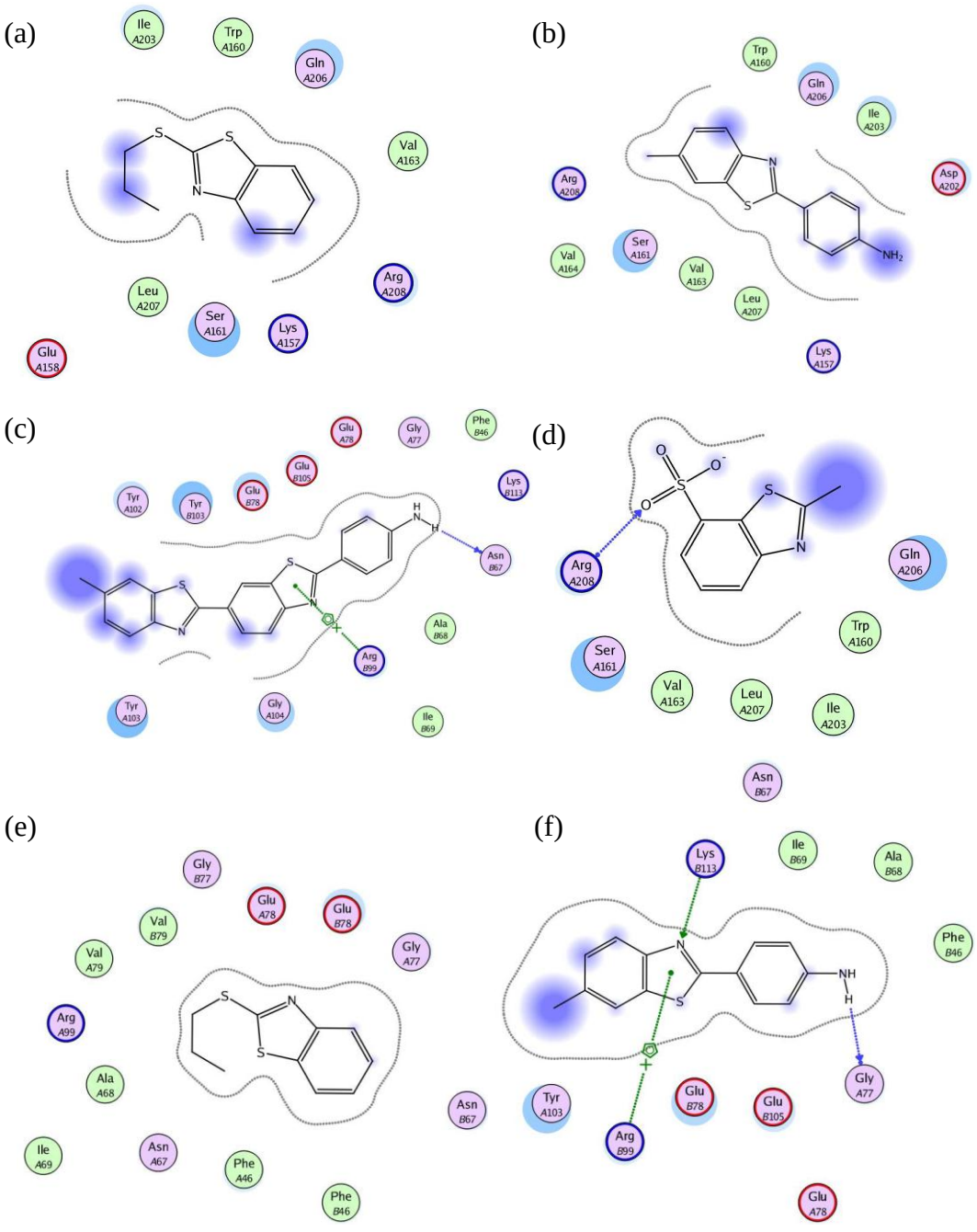

Figure 4.16. Derivatives of ligands on D3: (a) D3- Derivative of ligand 8, (b) D3- Derivative of ligand 9, (c) D3- Derivative of ligand 10, (d) D3- Derivative of ligand 2, (e) D3- Derivative of ligand 8 (2^{nd} cluster), (f) D3- Derivative of ligand 9 (2^{nd} cluster)

4.4 Blind hTIM Dimer Dockings

In the previous interface aimed docking study, Ligands 8 and 9 were docked both hTIM and TcTIM to investigate the differences between binding poses and affinities on the interface region. It is reported that, due to the different conformational arrangements of aromatic clusters on interface region of both TcTIM and hTIM, large benzothiazoles could not be accommodated in hTIM interface (Espinoza-Fonseca and Trujilo-Ferrara, 2005).

In the present study different methodology (blind docking methodology) was applied for hTIM dockings in order to invesitgate the selectivity for interface region of inhibitory ligands and compare the binding modes in TcTIM and hTIM cases. Ligands 8, 9 and 10 was docked to hTIM conformers (H1, H2 and H3). The analysis for the blind hTIM dimer dockings were carried out for the conformations that exist within the 1kcal/mol of the lowest energy conformation for H1, H2 and H3.

As seen in Figure 4.17, the inhibitor ligand 8 does not prefer to bind the interface of hTIM in the lowest energy conformations of H1, H2 and H3. Ligand 8 makes H-bonding with Lys159, Lys32, and Asn11 in its lower energy conformations on H1, H2 and H3 respectively (Figure 4.18). On the other hand, ligands 9 binds to the interface in the lowest energy conformations on H1 and H3 respectively and it makes H-bonding with Gly76 and cation-π interactions with Arg98 and Lys112 (Figure 4.19 (a)). However, the sulfonate group of ligand 9 does not make specific interactions with receptor interface residues contrary to the results in TcTIM dimer case. Similarly, Ligand 10 binds to the interface in H3 and makes H-bonding with Lys 68, Glu104, Gln111 and there are also cation-π interactions with Arg98 and Phe102 (Figure 4.20 (c)).

(a)

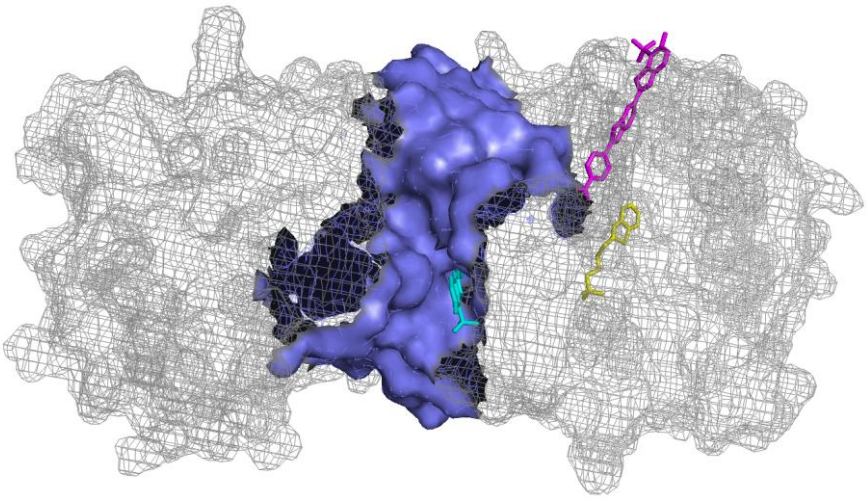

(b)

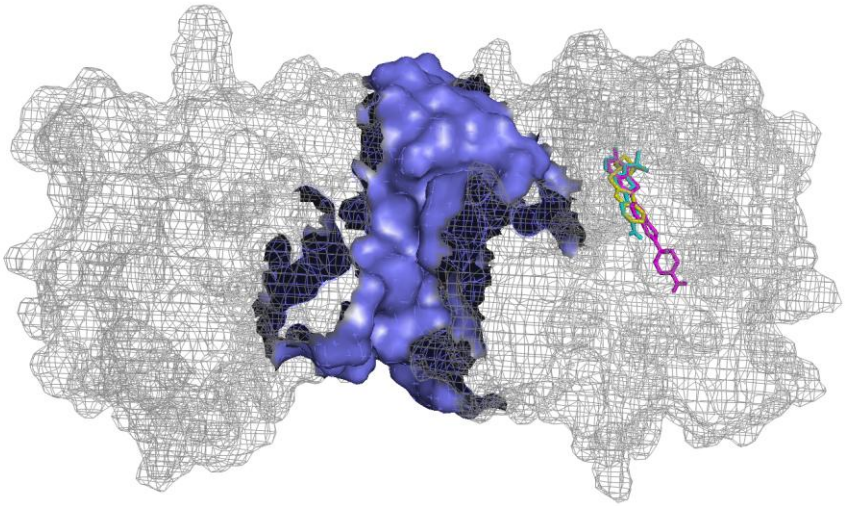

(c)

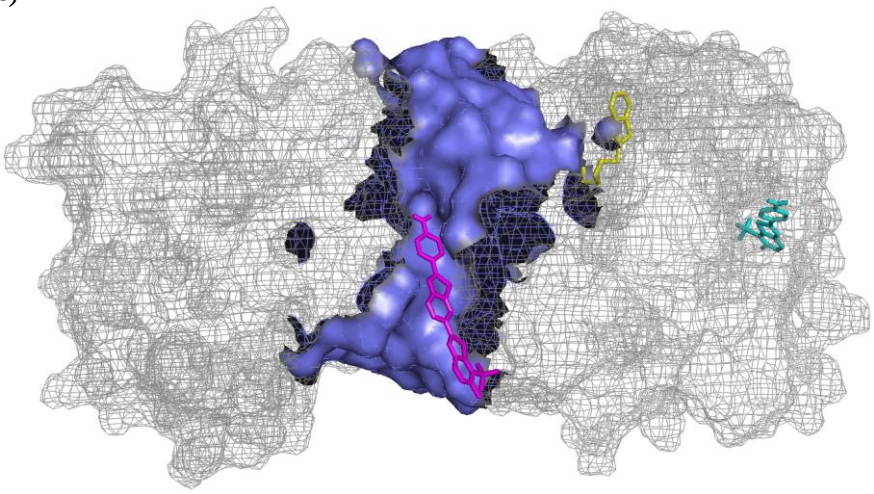

Figure 4.17. hTIM dimer dockings: Lowest energy conformations for (a) H1, (b) H2, (c) H3. The interface region is shown as “surface” (color: purple) together with ligand 8 (yellow), ligand 9 (cyan) and ligand 10 (magenta)

(a)

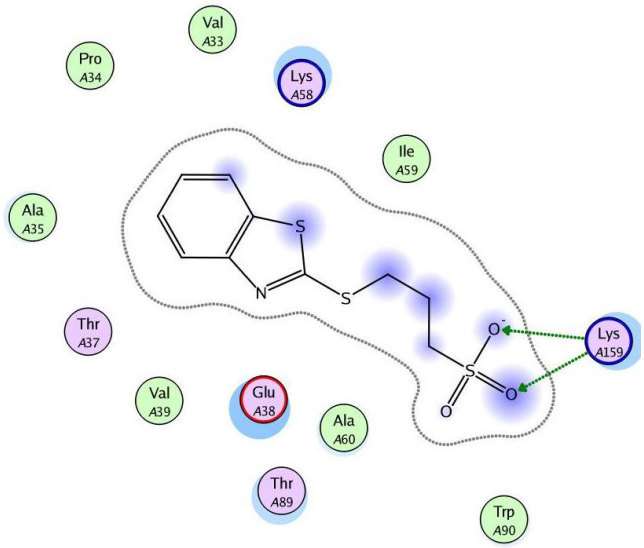

(b)

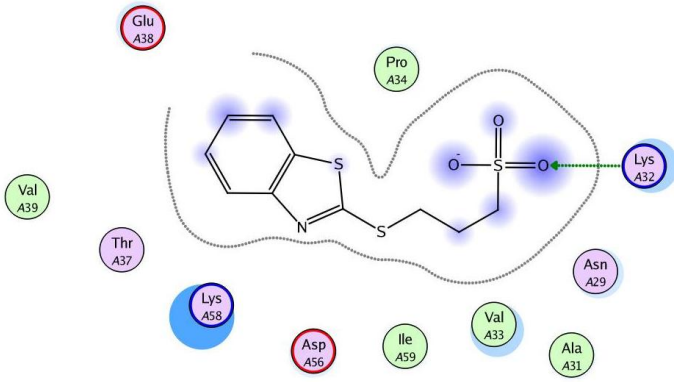

(c)

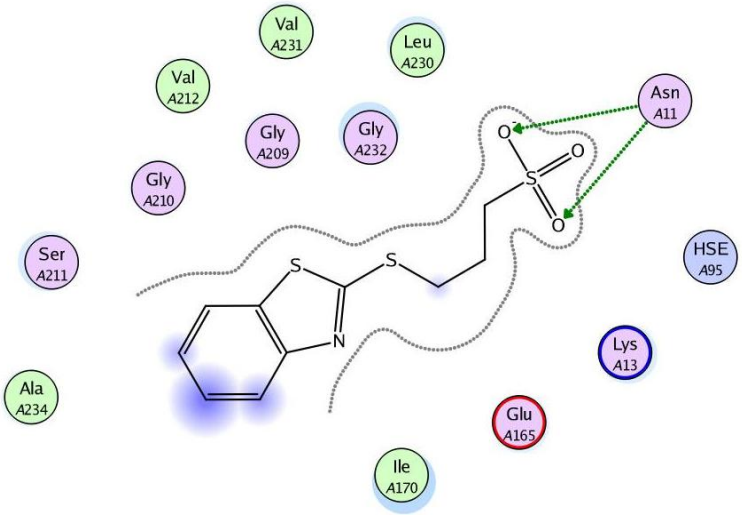

Figure 4.18. hTIM dimer dockings: MOE 2D diagrams indicating the interactions between ligand 8 and surrounding residues within 4.5 Å at the lowest energy conformations. H1-ligand 8, (b) H2-ligand 8, (c) H3-ligand 8

(a)

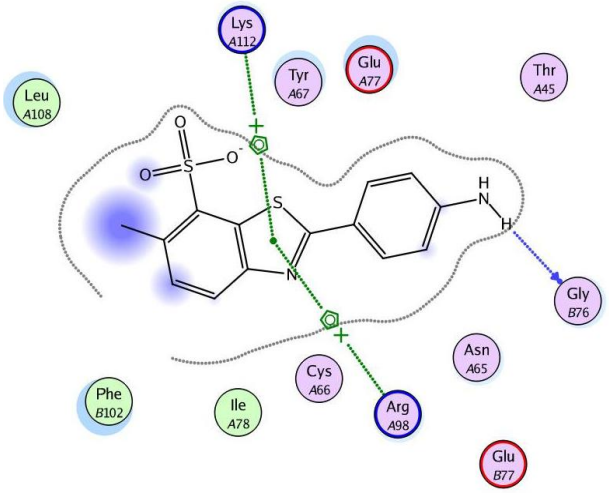

(b)

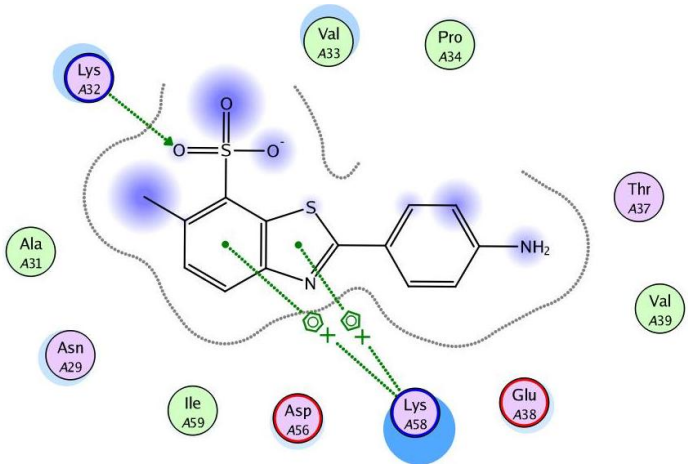

(c)

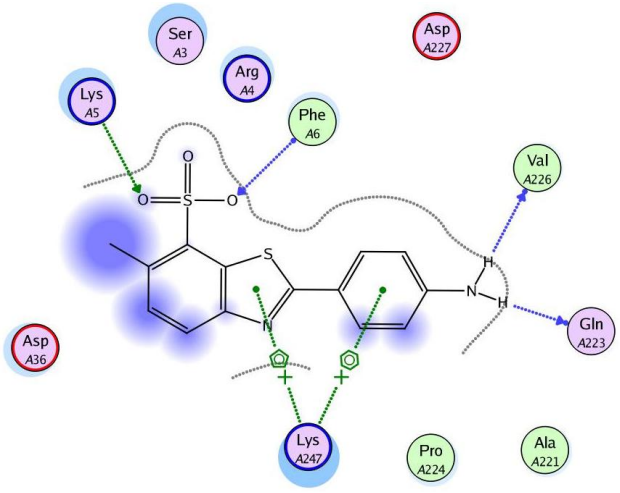

Figure 4.19. hTIM dimer dockings: MOE 2D diagrams indicating the interactions between ligand 9 and surrounding residues within 4.5 Å at the lowest energy conformations. (a) H1-ligand 9, (b) H2-ligand 9, (c) H3-ligand 9

(a)

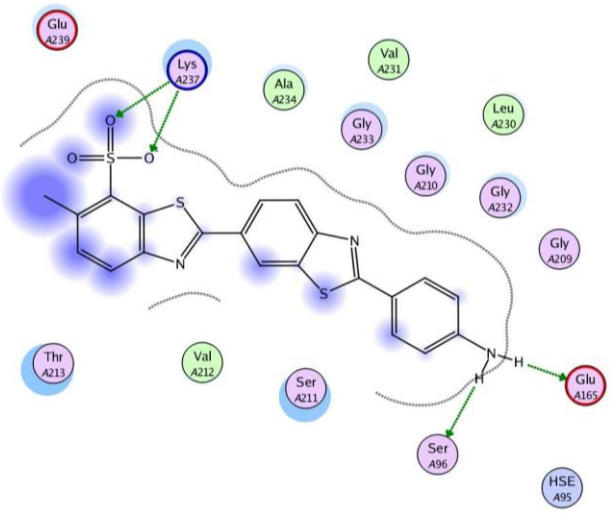

(b)

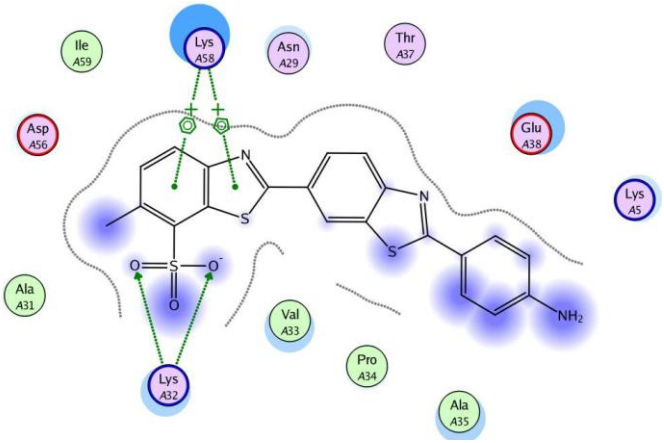

(c)

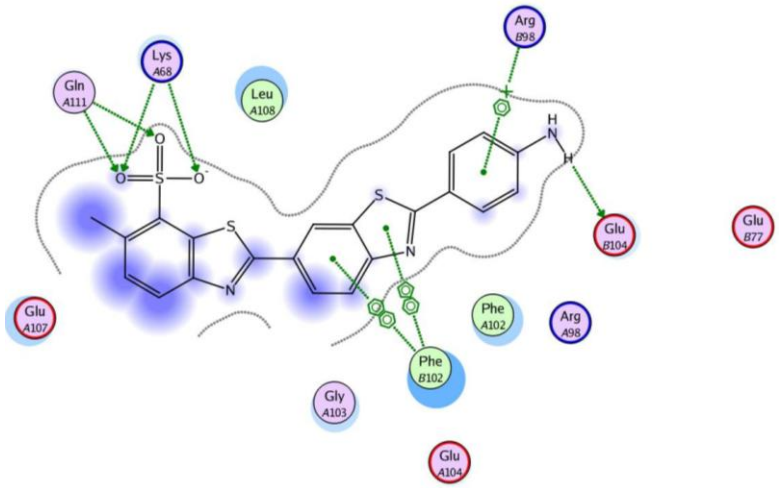

Figure 4.20. hTIM dimer dockings: MOE 2D diagrams indicating the interactions between ligand 10 and surrounding residues within 4.5 Å at the lowest energy conformations. (a) H1-ligand 10, (b) H2-ligand 10, (c) H3-ligand 10.

Table 4.5. Docking scores and the number of occurrences at the interface for hTIM dimer dockings

Dimer Dockings	D1	D2	D3	Fraction of Occurrence at interface	Fraction of Occurrence at interface (weighted)
	ΔG (kcal/mol) (Cluster #)	ΔG (kcal/mol) (Cluster #)	ΔG (kcal/mol) (Cluster #)		
Ligand 8	- 7.54 (2nd)	-6.94 (3rd)	-6.98 (1st)	27/97=0.28	0.22
Ligand 9	- 6.98 (1st)	-	-6.10 (2nd)	44/165=0.27	0.15
Ligand 10	- 8.25 (2nd)	-	-8.01 (1st)	78/131=0.60	0.32

Lowest free energy of binding for ligands at the interface and the percentage of the conformations (within 1 kcal/mol) that lie at the interface region are listed in Table 4.5. The ligands 8, 9 and 10 bind TcTIM interface more frequently than hTIM interface. The percentage values of ligands 8, 9 and 10 in TcTIM were found as 74%, 89% and 89%, respectively (Table 4.2). These values are higher compared to 28%, 27% and 60% in hTIM. The high percentage value of 60% for ligand 10 in hTIM case is caused by the fact that ligand 10 often selects the interface region in the last snapshot (H3). However this snapshot belongs to the cluster of the MD trajectory that has the fewest number of conformations, i.e., the least sampled conformation. To avoid this overestimation, the percentages was further weighted by the number of elements in the cluster that the snapshot belongs to. The corrected values then become 22%, 15% and 32% for ligands 8, 9 and 10, respectively. Low occurrence percentages at the interface region (last column in Table 4.5) clearly indicate that the interface of hTIM is not the primary binding site preferred by the inhibitors. This result can be verified form the illustrated occurrence density figures (in which the color code runs approximately from blue (0-12 %), light blue (13-24%), cyan (25-36%), green (37-48%), yellow (49-60%), orange (61-72%) to red (73-84%)) and plots (Figures 4.21 and 4.22, respectively) from which high occurrence density of inhibitors at the non-interface part of the enzyme can be observed. In other words, inhibitors rarely bind to interface region on hTIM (Figure 4.21) and compared to hTIM, interface of TcTIM presents more favorable binding site for the inhibitors.

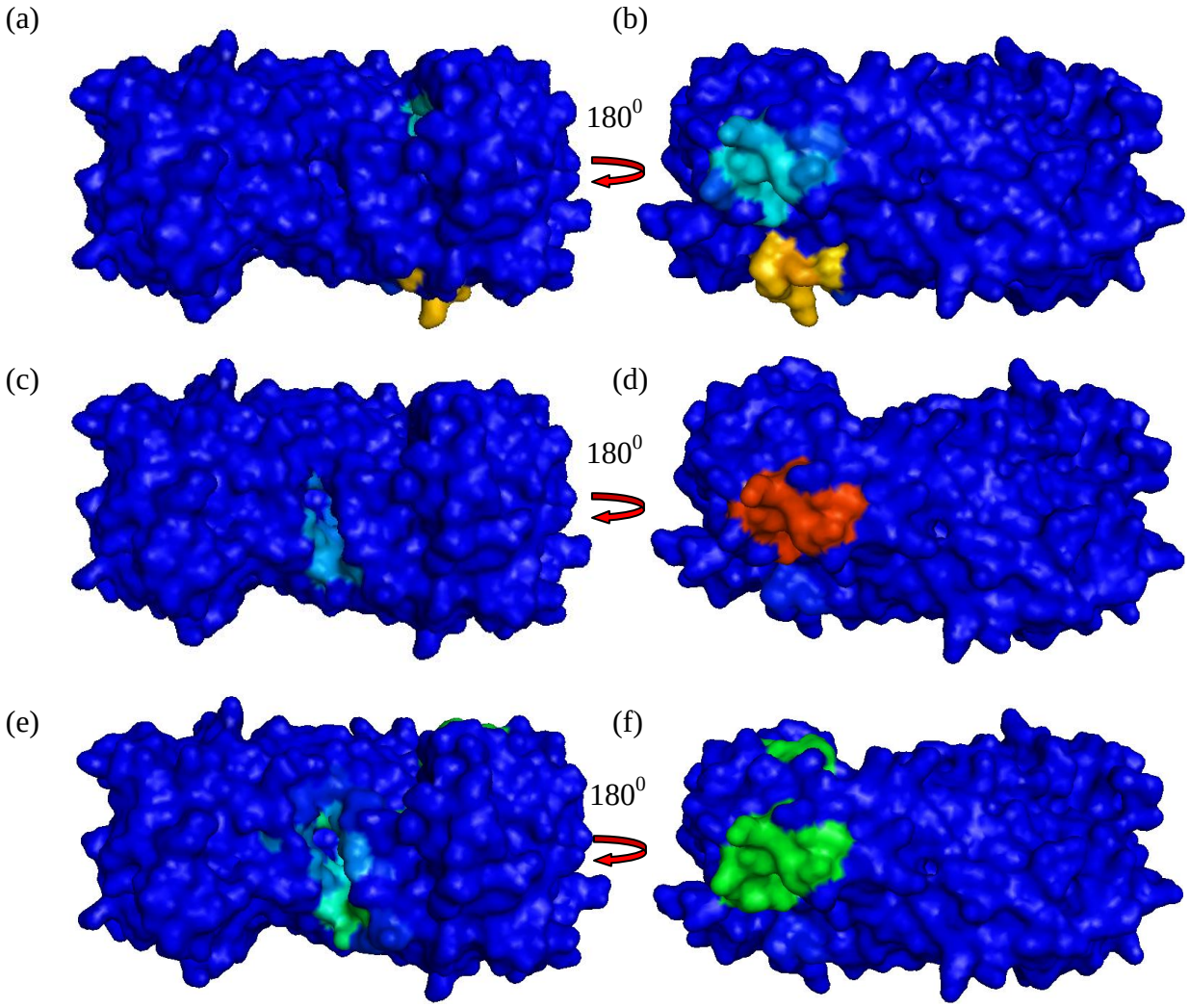

Figure 4.21. Occurrence density (weighted) figures for ligand 8 (a-b), ligand 9 (c-d) and ligand 10 (e-f).

(a)

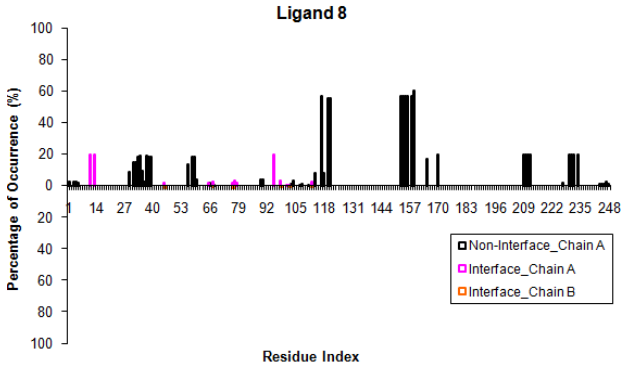

(b)

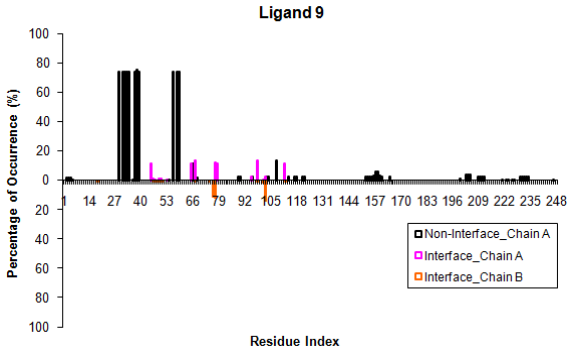

(c)

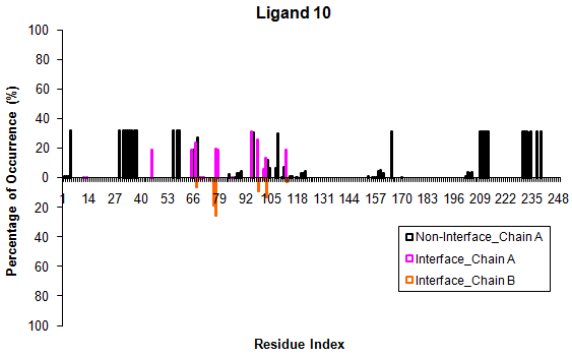

Figure 4.22. Percentage values of occurrence (weighted) graphs for hTIM dimer residues at a distance of 4.5 Å to ligand, (a) ligand 8, (b) ligand 9, (c) ligand 10

4.5 Binding Sites on TcTIM and hTIM Dimer

Table 4.6. Ligands' binding sites on TcTIM (with occurrence percentages of ligands)

Ligand	(1) Tunnel shaped cavity on the interface (loop 3, Tyr102-Thr106, Lys113)	(2) Catalytic site (Lys14, His96, Glu168)	(3) Lys53, Leu56-Asn58, Phe61-Ile63, Tyr87-Ser90	(4) Lys157-Val163, Arg208	(5) Glu19, His48-Met51, Ile83, Asp86	(6) Other
2	12	0	11	30	4	43
3	22	3	40	25	6	4
8	48	19	26	7	0	0
9	74	5	14	7	0	0
10	89	11	0	0	0	0

Occurrence percentages on preffered binding sites (on TcTIM) of ligands are listed in Table 4.6 and these binding sites are shown with different colors in Figure 4.23. The occurrence percentage values for tunnel shaped cavity on interface, are different from the values in Table 4.2 (last column), since calculations in Table 4.2, are based on the whole interface region. However, in Table 4.6 (second column), calculations are made for only tunnel shaped cavity on the interface region. As expected, higher binding percentages appear in the tunnel shaped cavity on TcTIM dimer interface for inhibitory ligands 8, 9 and 10 (48%, 74%, 89%, respectively) compared to ligands 2 and 3 (12% and 22%, respectively). This clearly indicates the significance of this region for the inhibition process. The distinguishing mark of ligand 10 is concentrating only on two sites: tunnel shaped cavity on the interface and the catalytic site, whereas ligands 8 and 9 also select different binding sites (especially ligand 8). This result may be consisted with the IC_{50} values listed in Table 2.2, which were 33 μM, 56 μM, 8 μM for ligands 8, 9 and 10 respectively. Therefore, the lowest IC_{50} value for ligand 10 may be related with its selective behavior for the interface region. Ligand 2 tends to bind different sites on TcTIM and does not concentrate on particular binding sites unlike other ligands.

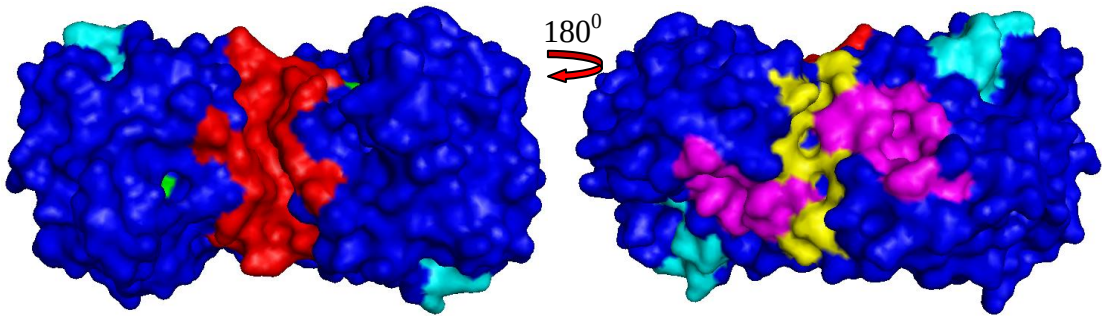

Figure 4.23. Binding sites on TcTIM : (1) red, (2) green, (3) magenta, (4) cyan, (5) yellow, and (6) blue

Table 4.7. Inhibitory ligands' binding sites on hTIM (with weighted occurrence percentages of ligands)

Ligand	(1) Cavity on the interface (loop 3, Val101, Phe102, Lys112)	(2) Catalytic site (Lys13, His95, Glu165)	(3) Ala31-Val39, Ile244-Gln248	(4) Asn153-Lys159, Ser203-Arg205	(5) Other
8	3	19	21	57	0
9	14	3	75	8	1
10	32	31	32	1	4

In Table 4.7, occurrence percentages on preffered binding sites (on hTIM) of the inhibitors, are listed and these binding sites are shown with different colors in Figure 4.24. Contrary to TcTIM results, inhibitory ligands do not select the cavity on the interface region as often as they did in the TcTIM dimer case. According to the IC_{50} values listed in Table 2.2 for hTIM case, ligand 9 is the weakest inhibitor for hTIM. Therefore, ligand 9's selectivity for the region Ala31-Val39, Ile244-Gln248 (75%), suggests that this region has no role in the inhibition process. In addition, ligand 8 that has the lowest IC_{50} value, binds

to the region consisting of Asn153-Lys159, Ser203-Arg205 in 57% of the conformations. Hence, this region might have a role in the inhibition process of the hTIM. The difference in IC_{50} values of ligands 9 and 10 might be due to the ligand 10's tendency to bind to cavity on the interface and catalytic site more often compared to ligand 9. Although, ligand 10 binds to cavity on the interface with high percentage (32%), it resides in a perpendicular manner (Figure 4.25) on interface at 58% of these conformations.

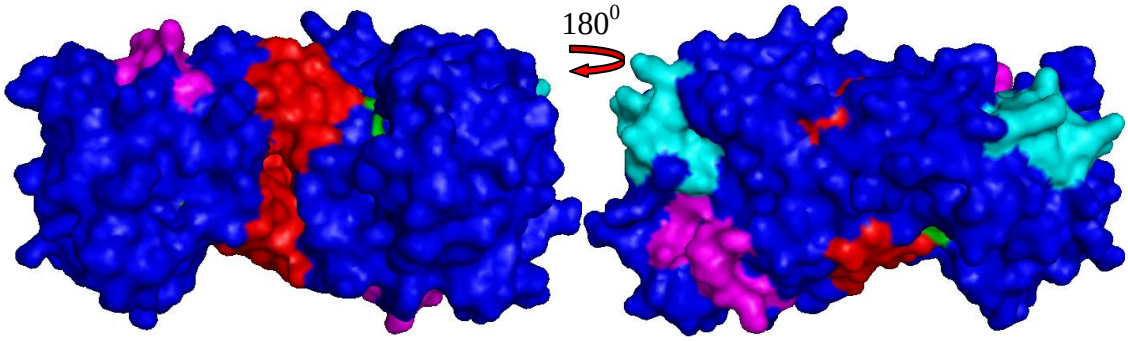

Figure 4.24. Binding sites on hTIM : (1) red, (2) green, (3) cyan and (4) magenta

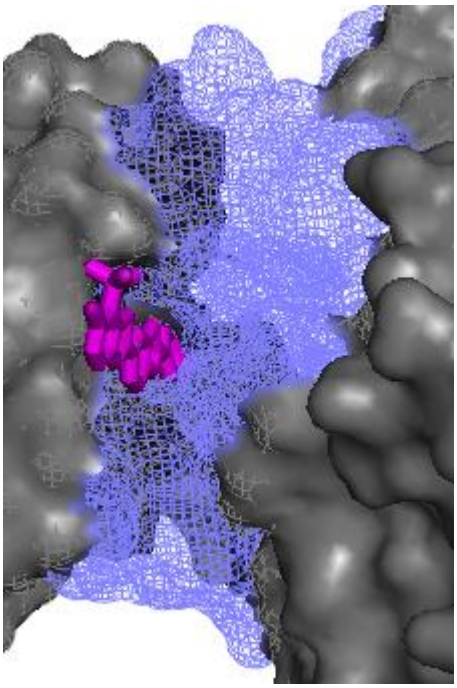

Figure 4.25. Perpendicular binding orientation of ligand 10 (magenta) on H1 conformer: The interface region is shown as "meshed" (color: purple).

5. CONCLUSIONS AND RECOMMENDATIONS

The computational studies on TcTIM have so far focussed on docking of the benzothiazoles to the constricted region of the interface between subunits. In the present study, the differences in the binding modes of ligands for TcTIM monomer, TcTIM dimer and hTIM dimer, are investigated using blind docking methodology with multiple receptor conformations. Main chain flexibility is incorporated via these different conformers obtained from MD simulations.

The comparison of TcTIM monomer and dimer docking results suggests that the tunnel shaped cavity on the interface region of dimeric form presents a more favorable binding site for the inhibitory ligands (8,9 and 10) than the interface region opened up in monomeric form. The inhibitory ligands prefer binding to the interface region of TcTIM, unlike non-inhibitory ligands (ligands 2 and 3). In TcTIM dimer dockings, strong inhibitors make π-π interactions with aromatic Phe75, Tyr102 and Tyr103, cation-π interactions with Arg71, Arg99 and Lys113 on the interface region. Furthermore, inhibitory ligands make H-bonding especially with the residues Asn67, Arg 99, Lys 113 by means of their sulfonate group.

In order to investigate the role of sulfonate group in the inhibiton process, dockings of sulfonate-free ligands (ligands 8,9 and 10) and sulfonate-added ligand 2 derivatives on D3 conformer were carried out. The results show that, selectivity for the interface region of the inhibitory ligand 10 is diminished by deletion of the sulfonate group. Meanwhile, addition of the sulfonate group to non-inhibitory ligand 2 increases the selectivity. These differences in selectivity for the interface region, might indicate that sulfonate group has a role in selective molecular recognition. Apart from this, derivatives of the inhibitory ligands 8, 9 and 10 tend to reside in a perpendicular manner on interface. However, original ligands prefer a binding pose in a planar manner on sinterface.

To estimate the differences in binding poses of the inhibitors on TcTIM and hTIM, blind dockings of ligands 8,9 and 10 on H1, H2 and H3 were performed. In view of comparison between the docking results on hTIM and TcTIM, we can state that the

interface of TcTIM dimer is more favorable binding site than interface of hTIM dimer for the inhibitory ligands. Moreover, low occurrence percentage values on the interface of hTIM, show that this region is not primary sbinding site for the inhibitors.

The analysis of different binding sites on TcTIM and hTIM, verifies the significance of the tunnel shaped cavity on TcTIM dimer interface for the inhibition process. Besides this, the results show that, the region consisting of Ala31-Val39, Ile244-Gln248 on hTIM has no effect in the inhibition process, whereas the region includes Asn153-Lys159, Ser203-Arg205 might have a role in the inhibition of hTIM dimer.

In the future, further MD simulations on ligand-bound forms of TcTIM and hTIM dimer can be performed to analyze the stability of complexes docked inhibitory ligands with TcTIM and to observe any changes in interactions and dynamics compared to the apo form. The comparison between dynamics of apo and holo forms, might reveal the structural dynamics of the inhibition process.

APPENDIX A: INTERFACE RESIDUES

Table A.1. Interface Residues of TcTIM and hTIM

TcTIM		**hTIM**	
Residue Name and Number	SASA Difference	Residue Name and Number	SASA Difference
ASN 12	4.82	ASN 11	6.50
TRP 13	0.33	LYS 13	35.57
LYS 14	24.87	MET 14	176.71
CYS 15	122.41	ASN 15	30.74
ASN 16	39.80	GLY 16	6.53
GLY 17	8.28	ARG 17	110.38
SER 18	20.06	LYS 18	67.58
GLU 19	27.26	GLN 19	1.27
SER 20	1.40	PRO 44	17.18
THR 45	27.97	THR 45	63.21
PHE 46	72.58	ALA 46	86.27
LEU 47	151.28	TYR 47	36.05
HIS 48	29.39	ILE 48	5.20
ILE 49	5.68	ASP 49	50.49
PRO 50	35.39	PHE 50	4.15
MET 51	1.84	GLN 53	3.74
GLN 66	33.77	GLN 64	39.75

Table A.2. Interface Residues of TcTIM and hTIM (cont'd)

TcTIM		hTIM	
Residue Name and Number	SASA Difference	Residue Name and Number	SASA Difference
ASN 67	7.30	ASN 65	9.01
ALA 68*	0.00	TYR 67	19.00
ILE 69	11.57	VAL 69	1.48
THR 70*	0.00	THR 70	9.89
ARG 71	0.16	ASN 71	38.49
SER 72	19.50	GLY 72	23.19
GLY 73	35.31	ALA 73	38.56
ALA 74	37.62	PHE 74	73.83
PHE 75	83.62	THR 75	129.53
THR 76	145.31	GLY 76	44.56
GLY 77	66.11	GLU 77	59.60
GLU 78	67.02	ILE 78	24.57
VAL 79	25.93	SER 79	3.79
SER 80	2.29	GLY 81	14.98
GLN 82	0.13	MET 82	89.62
ILE 83	92.83	ILE 83	0.70
LEU 84	8.00	ASP 85	75.69
ASP 86	57.85	CYS 86	36.75
TYR 87	46.19	VAL 92	0.66

Table A.3. Interface Residues of TcTIM and hTIM (cont'd)

TcTIM		hTIM	
Residue Name and Number	SASA Difference	Residue Name and Number	SASA Difference
ILE 89	0.17	HIS 95	9.30
VAL 93	1.09	GLU 97	28.81
HIS 96	8.78	ARG 98	39.96
GLU 98	37.61	VAL 101	25.77
ARG 99	45.59	PHE 102	69.21
TYR 102	26.91	LYS 112	0.22
TYR 103	73.63		
GLY 104*	0.00		
GLU 105	3.10		
THR 106*	0.00		
LYS 113	0.25		

*Residues determined by visualization.

REFERENCES

Albery J and JR Knowles, 1976, "Free-Energy Profile for the Reaction Catalyzed by Triosephosphate Isomerase", *Biochemistry*, Vol. 15, No. 25, pp. 5627-5631.

Akten, E. D., S. Cansu, and P. Doruker, 2009, "A Docking Study Using Atomistic Conformers Generated via Elastic Network Model for Cyclosporin A/Cyclophilin A Complex", *Journal of Biomolecular Structure & Dynamics*, Vol. 27, pp. 13-25.

Berendsen, H. J. C., J. P. M. Postma, W. F. van Gunsteren, A. DiNola, and J. R. Haak, 1984, "Molecular dynamics with coupling to an external bath", *Journal of Chemical Physics*, Vol. 81, pp. 3684-3690.

Cansu, S., and P. Doruker, 2008, "Dimerization Affects Collective Dynamics of Triosephosphate Isomerase", *Biochemistry*, Vol. 47, pp. 1358-1368.

Case, D. A., T. A. Darden, T. E. Cheatham, C. L. Simmerling, J. Wang, R. E. Duke, R. Luo , K. M. Merz, B. Wang, D. A. Pearlman, M. Crowley, S. Brozell, V. Tsui, H. Gohlke, J. Mongan, J. V. Hornak, G. Cui, P. Beroza, C. Schafmeister, J. W. Caldwell, W. S. Ross, and P. A. Kollman, 2004, *AMBER 8*, University of California, San Francisco.

Case, D. A., T. E. Cheatham, T. A. Darden, H. Gohlke, R. Luo, K. M. Merz, Jr. A. Onufriev, C. Simmerling, B. Wang, and R. Woods, 2005, "The Amber biomolecular simulation programs", *Journal of Computational Chemistry*, Vol. 26, pp. 1668-1688.

Cavasotto, C. N., and R. A. Abagyan, 2004, "Protein Flexibility in Ligand Docking and Virtual Screening to Protein Kinases", *J. Mol. Biol.*, Vol. 337, pp. 209-225.

Cavasotto, C. N., J. A. Kovacs, and R. A. Abagyan, 2005, **"**Representing receptor flexibility in ligand docking through relevant normal modes", *JACS*, Vol. 127, pp. 9632-9640.

Clark, A. M., P. Labute, M. Santavy, 2006, "2D Structure Depiction", *Journal of Chemical Information and Modeling*, Vol. 46, pp. 1107-1123.

Delano, W. L., 2002, "The PyMOL Molecular Graphics System", *DeLano Scientific*, Palo Alto, CA, USA.

Duan, Y., C. Wu, S. Chowdhury, M. C. Lee, G. Xiong, W. Zhang, R. Yang, P. Cieplak, R. Luo, and T. Lee, 2003, " A Point charge force field for molecular mechanics simulations of proteins", *Journal of Computational Chemistry*, Vol. 24, pp. 1999-2012.

Espinoza-Fonseca, L. M., and J. G. Trujillo-Ferrera, 2004, "Exploring the possible binding sites at the interface of triophosphate isomerase dimer as potential target for anti-tripanosomal drug design", *Bioorganic and Medicinal Chemistry Letters,* Vol. 14, pp. 3151-3154.

Espinoza-Fonseca, L.Michel, and Jose G. Trujillo-Ferrera, 2005, "Structural considerations for the rational design of selective anti-trypanosomal agents: The role of the aromatic clusters at the interface of triophosphate isomerase dimer", *Biochemical and Biophysical Research Communications*, Vol. 328, pp. 922-928.

Espinoza-Fonseca, L.Michel, and Jose G. Trujillo-Ferrera, 2006, "Toward a rational design of selective multi-trypanosomatid inhibitors: A computational docking study", *Bioorganic and Medicinal Chemistry Letters,* Vol. 16, pp. 6288-6292.

Essmann, U., L. Perera, M. L. Berkowitz, T. Darden, H. Lee, and L. G. Pedersen, 1995, "A smooth particle mesh Ewald method," *Journal of Chemical Physics*, Vol. 103, pp. 8577-8593.

Feller, S. E., Y. H. Zhang, R. W. Pastor, and B. R. Brooks, 1995, "Constant pressure molecular dynamics simualtions – the Langevin piston method", *Journal of Chemical Physics*, Vol. 103, pp. 4613-4621.

Gao, XG., E. Maldonado, R. Perez-Monfort, G. Garza-Ramos, M. T. Gomez-Puyou, A. Gomez-Puyou, and A. Rodriguez-Romero, 1999, "Crystal structure of triosephosphate isomerase from Trypanosoma cruzi in hexane", *Biochemistry*, Vol. 96, pp. 10062-10067.

Garza-Ramos, G., R. Perez Montfort, A. Rojo-Dominguez, M. T. de Gomez-Puyou, A. Gomez-Puyou, 1996, "Species-specific inhibition of homologous enzymes by modification of non-conserved amino acids residues. The cysteine residues of triosephosphate isomerase.", *European Journal of Biochemistry*, Vol. 241, pp. 114-120.

Gayosso-De-Lucio, J., M. Torres-Valencia, A. Rojo-Dominguez, H. Najera-Pena, B. Aguirre-Lopez, J. Salas-Pacheo, C. Avitia-Dominguez, and A. Tellez-Valencia, 2009, "Selective Inactivation of triosephosphate isomerase from Trypanosoma cruzi by brevifolin carboxylate derivatives isolated from Geranium bellum Rose", *Bioorganic and Chemistry Letters*, Vol. 19, pp. 5936-5939.

Gomez Puyou, A., E. Saavedra-Lira, I. Becker, R. A. Zubillaga, A. Rojo-Dominguez, and R. Perez-Montfort, 1995, "Using evolutionary changes to achieve species-specific inhibition of enzyme action – studies with triosephosphate isomerase", *Chemistry & Biology*, Vol. 2, pp. 847-855.

Goodford, P. J., 1984, " A Computational Procedure for Determining Energetically Favorable Binding Sites on Biologically Important Molecules", *Journal of Medical Chemistry*, Vol. 28, pp. 849-857.

Goodsell, S. D., G. M. Morris, and A. J. Olson, 1996, "Automated Docking of Flexible Ligands: Applications of Autodock", *Journal of Molecular Recognition*, Vol. 9, pp. 1-5.

Gray, J. J., S. Moughon, C. Wang, O. Schueler-Furman, B. Kuhlman, and D. Baker, 2003, "Protein-protein docking with simultaneous optimization of rigid-body displacement and side-chain conformations", *J. Mol. Biol.*, Vol. 33, pp. 281-299.

Hernandez-Alacantara, G., G. Garza-Ramos, G. M. Hernandez, A. Gomez-Puyou, R. Perez-Montfort, 2002, "Catalysis and stability of triosephosphate isomerase from Trypanosoma brucei with different residues at position 14 of the dimer interface. Characterization of a catalytically component monomeric enzyme", *Biochemistry*, Vol. 41, pp. 4230-4328.

Hetenyi, C., and D. van der Spoel, 2002, "Efficient docking of peptides to proteins without prior knowledge of the binding site", *Protein Science*, Vol.11, 1729-1737.

Hockney, R. W., 1970, "The Potential Calculations on Some Applications", *Methods in Computational Physics*, Vol. 9, pp. 136-143.

Huey, R., G. M. Morris, A. J. Olson, and D. S. Goodsell, 2007, "Software news and update: A semiempirical free energy force field with charge-based desolvation", *Journal of Computational Chemistry*, Vol. 28, pp. 1145-1152.

Humphrey, W., A. Dalke, and K. Schulten, 1996, "VMD: visual molecular dynamics", *Journal of Molecular Graphics and Modelling*, Vol. 14, pp. 27-33.

Jorgensen, W. L., J. Chandrasekhar, J. D. Madura, R. W Impey, and M. L. Klein, 1983, "Comparison of simple potential functions for simulating liquid water", *Journal of Chemical Physics*, Vol. 79, pp. 926-935.

Kempf, J. G., J. Y. Jung, C. Ragain, N. S. Sampson and J. P. Loria, 2007, "Dynamic requirements for a functional protein hinge", *Journal of Molecular Biology*, Vol. 368, pp. 131-149.

Knegtel, R. M. A., I.D. Kuntz, and C. M. Oshiro, 1997, "Molecular Docking to Ensembles of Protein Structures", *Journal of Molecular Biology*, Vol. 266, pp. 424-440.

Lamarck, J. B., 1914, *Zoological Philosophy*, Macmillan, London.

Leach, A. R., 2001, *Molecular Modelling: Principles and Applications (2nd edition)*, Prentice Hall.

Lloyd, P. Stuart, 1982, "Least squares quantization in PCM", *IEEE Transactions on Information Theory*, Vol. 28, pp. 129-137.

MacKerell, A. D., Jr., D. Bashford, M. Bellott, R. L. Jr. Dunbrack, J. Evanseck, M. J. Field, S. Fischer, J. Gao, H. Guo, S. Ha, D. Joseph, L. Kuchnir, K. Kuczera, F. T. K. Lau, C. Mattos, C. Michnick, T. Ngo, D. T. Nguyen, B. Prodhom, I. W. E. Reiher, B. Roux, M. Schlenkrich, J. Smith, R. Stote, J. Straub, M. Watanabe, J. Wiorkiewicz-Kuczera, D. Yin, and M. Karplus, 1998, "All-hydrogen empirical potential for molecular modeling abd dynamic studies of proteins using the CHARMM22 force field", *The Journal of Physical Chemistry*, Vol. 102, pp. 3586-3616.

MacKerell, A. D., Jr., D. Bashford,M. Bellott; R. L. Jr. Dunbrack, J. Evanseck, M. J. Field, S. Fischer, J. Gao, H. Guo, S. Ha., Joseph D., L. Kuchmir, K. Kuczera, F. T. K. Lau, C. Mattos, S. Michnick, T. Ngo, D. T. Nguyen, B. Prodhom, B. Roux, M. Schlenkrich, J. Smith, R. Stote, J. Straub, M. Watanabe, J. Wiorkiewicz-Kuczera, D. Yin, and M. Karplus, 1992, "Self-consistent parameterization of biomolecules for molecular modeling and condensed phase simulations", *The FASEBJ Journal*.

Mainfroid, V., P. Terpstra, M. Beauregard, J. M. Frere, S. C. Mande, W. G. J. Hol, J. A. Martial, and K. Goraj, 1996, "Three hTIM Mutants that Provide New Insights on why TIM is a Dimer", *J. Mol. Biol*., Vol. 257, pp. 441-456.

Maldonado, E., M. Soriano-Garcia., A. Moreno, N. Cabrera, G. Garzo-Ramos, M. Gomez-Puyou, A. Gomez Puyou, and R. Perez-Montfort, 1998, "Differences in the Intersubunit Contacts In Triosphosphate Isomerase from Two Closely Related Pathogenic Trypanosomes", *Journal of Molecular Biology*, Vol. 283 , pp. 193-203.

Meiler, J., and D. Baker, 2006, "ROSETTALIGAND: Protein Small Molecule Docking with Full Side-Chain Flexibility", *Proteins*, Vol. 65, pp. 538-548.

M, Gerstein,1992, "A Resolution-Sensitive Procedure for Comparing Protein Surfaces and its Application to the Comparison of Antigen-Combining Sites," *Acta Crystallographica*, A48, pp. 271-276.

Michael Feig, John Karanicolas, Charles L. Brooks, III: MMTSB Tool Set, 2001, MMTSB NIH Research Resource, The Scripps Research Institute.

Morris, G. M., R. Huey, W. Lindstrom, M. F. Sanner, R. K. Belew, D. S. Goodsell, and A. J. Olson, 2009, "AutoDock4 and AutoDockTools4: Automated Docking with Selective Receptor Flexibility", *J. Comput. Chem.*, Vol. 30, pp. 2785–2791.

Morris, G. M., S. D. Goodsell, R. S. Halliday, R. Huey, W. E. Hart, R. K. Belew, and A. J. Olson, 1998, "Automated Docking Using Lamarckian Genetic Algorithm and an Empirical Binding Free Energy Function", *Journal of Computational Chemistry*, Vol. 19, pp. 1639-1662.

Olivares-Illana, V., R. Perez Montfort, F. Lopez-Callohara, M. C. A. Rodriguez-Romero, M. T. Gomez-Puyou, and A. Gomez-Puyou, 2006, "Structural Differences in Triosephosphate Isomerase from Different Species and Discovery of a Multitrypanosomid Inhibitor", *Biochemistry*, Vol. 45, pp. 2556-2560.

Olivares-Illana, V., A. Rodriguez-Romero, I. Becker, M. Berzunza, J. Garcia, R. Perez-Montfort, N. Cabrera, F. Lopez-Calahorra, M. T. Gomez Puyou, and A. Gomez-Puyou, 2007, "Perturbation of the Dimer Interface of Triosephosphate Isomerase and its Effect on Trypanosoma Cruzi", *PLOS Neglected Tropical Diseases*, Vol. 1, pp. 1-8.

Perez-Montfort, R., M. T. Gomez-Puyou, and A. Gomez-Puyou, 2002, "The Interfaces of Oligomeric Proteins as Targets for Drug Design against Enzymes from Parasites", *Current Topics in Medicinal Chemistry* , Vol. 2, pp. 457-470.

Phillips, J. C., R. Braun, W. Wang, J. Gumbart, E. Tajkhorshid, E. Villa, C. Chipot, R. D. Skeel, L. Kale, and K. Schulten, 2005, "Scalable molecular dynamics with NAMD", *Journal of Computational Chemistry*, Vol. 26, pp. 1781-180.

Pompliano, DL, A. Peyman, and JR. Knowles, 1990, "Stabilization of a reaction intermediate as a catalytic device: definition of the functional role of the flexible loop in triosephosphate isomerase." *Biochemistry*, Vol. 29, pp. 3186-3194.

Ryckaert, J. P., G. Ciccotti, and H. J. C. Berendsen, 1977, "Numerical integration of the Cartesian equations of motion of a system with constraints: Molecular dynamics of n-alkanes", Journal *of Computational Physics*, Vol. 23, pp. 327-341.

Sadowski, J., J. Gasteiger, and G. Klebe, 1994, "Comparison of Automatic Three-Dimensional Model Builders Using 639 X-Ray Structures", *J. Chem. Inf. Comput. Sci.*, Vol.34, pp. 1000-1008. The 3D structure generator CORINA is available from Molecular Networks GmbH, Erlangen, Germany (http://www.molecular-networks.com).

Schliebs, W., N. Thanki, R. Jaenicke, R. K. Wierenga, 1997, " A double mutation at the tip of the dimer interface loop of triosephosphate isomerase generates active monomers with reduced stability", *Biochemistry*, Vol. 36, pp. 9655-9662.

Schnackerz, K. D., and Gracy, R. W., 1991, "Probing the catalytic sites of triosephosphate isomerase by 31P-NMR with reversibly and irreversibly binding substrate analogs", *European Journal of Biochemistry*, Vol. 199, pp. 231-238.

Stouten, P. F. W., C. Frömmel , H. Nakamura, C. Sander, 1993, "An effective solvation term based an a atomic occupancies for use in protein simulations" *Molecular Simulaion*, Vol. 10, pp. 97–120.

Swope, W. C., Hans C. Andersen, Peter H. Berens and Kent R. Wilson, 1982, "A computer simulation method for the calculation of equilibrium constants for the formation of physical clusters of molecules: Application to small water clusters", *The Journal of Chemical Physics,* vol. 76, pp. 637-650.

Tellez-Valencia, A., S. Avila-Rios, R. Perez-Monfort, A. Rodriguez-Romero, M. T. Gomez-Puyou, F. Lopez-Calahora, and A. Gomez-Puyou, 2002, "Highly specific inactivation of triophosphate isomerase from Trypanosoma cruzi", *Biochemical and Biophysical Research Communications,*Vol. 295, pp. 958-963.

Tellez-Valencia, A., V. Oliveres-Illana, A. Hernandez-Santoyo, R. Perez-Montfort, M. C. A. Rodriguez-Romero, F. Lopez-Calahore, M. T. Gomez Puyou, and A. Gomez Puyou, 2004, "Inactivation of Triophosphate Isomerase from Trypanosoma cruzi by an Agent that Perturbs its Dimer Interface", *Journal of Molecular Biology*, Vol. 341, pp. 1355-1365.

Verlet, L., 1967, "Computer Experiments on Classical Fluids. I. Thermodynamical Properties of Lennard-Jones Molecules", *Physical Review*, Vol. 159, pp. 98-103.

Weiner, S. J., P. A. Kollman, D. A. Case, U. C. Singh, C. Ghio, G. Alagona, S. Profeta, and P. Weiner, 1984, "A new force field for molecular mechanical simulation of nucleic acids and proteins", *Journal of the American Chemical Society*, Vol.106, pp. 765-784.

Wierenga, R. K., M. E. M. Noble, G. Vriend, S. Nauche, and W. G. J. Hol., 1991, "Refined 1.83 Å structure of the trypanosomal triosephosphate isomerase crystallized in the presence of 2.4 m-ammonium sulfate.", *Journal of Molecular Biology* ,Vol. 220, pp. 995–1015.

Williams, J. C. and A. E. McDermott, 1995, "Dynamics of the flexible loop of triosephoshate isomerase: the loop motion is not ligand gated", *Biochemistry*, Vol. 34, pp. 8309-8319.

Xiang, J., J. Jung and N. S. Sampson, 2004, "Entropy effects on protein hinges: the reaction catalyzed by triosephosphate isomerase", *Biochemistry*, Vol. 43, pp. 11436-11445,.

Zacharias, M., 2004, "Rapid Protein-ligand docking including soft degrees of freedom from molecular dynamics simulations to account for protein flexibility: FK506 binding to FKBP binding protein as an example", *Proteins*, Vol. 54, pp. 759-767.

Zomosa-Signoret ,V., G. Hernandez-Alcantara, H. Reyes-Vivas, E. Martinez-Martinez, G. Garza-Ramos, R. Perez Montfort, M. Gomez-Puyou, and A. Gomez-Puyou, 2003, "Control of the Reactivation Kinetics of Homodimeric Triosephosphate Isomerase from Unfolded Monomers", *Biochemistry*, Vol. 42, pp. 3311-3318.